Prediction of future Alaskan lake methane emissions using a small-lake model coupled to a regional climate model

Daniela Hurtado Caicedo[1], Leon Boegman[1], Hilmar Hofmann[2] and Aidin Jabbari[3]

[1]Environmental Fluid Dynamics Laboratory, Department of Civil Engineering, Queen's University, Kingston, ON, Canada
[2]Environmental Physics Group, Limnological Institute, University of Konstanz, Konstanz, Germany
[3]Fisheries and Oceans Canada, Bedford Institute of Oceanography, Dartmouth, Nova Scotia, Canada

Corresponding author: first and last name (boegmanl@queensu.ca)

Key Points:

- CH_4 emissions from lakes are not presently in the land surface schemes of Global Climate Models
- A one-dimensional lake model was developed to simulate future CH_4 diffusive and ebullitive fluxes from four Arctic lakes
- Three climate warming scenarios simulated the bottom water temperature to warm by up to 2.24°C, increasing the surface CH_4 flux from the four lakes by 38 – 129%.

Abstract

Methane emissions from lakes will increase with climate warming. However, CH_4 emissions from lakes are not presently in the land surface schemes of Global Climate Models (GCMs). Modelled climate projections depend on future atmospheric CH_4 concentrations; therefore, a positive feedback loop is not simulated. To address this issue, a one-dimensional lake model was developed to simulate future CH_4 diffusive and ebullitive fluxes from four Arctic lakes. The model was hindcast for validation (1976-2005) and forecast for prediction (2071-2100) with one-way coupling to raw meteorological data from the CanESM2 ensemble GCM. Three climate warming scenarios (RCPs 2.6, 4.5 and 8.5) simulated the bottom water temperature to warm by up to 2.24°C, increasing the surface CH_4 flux from the four lakes by 38 – 129%. However, RCP 2.6 and 4.5 led to stabilized temperatures and CH_4 emissions by 2100, at levels of 0.63 – 1.21°C and 38 – 67%, respectively, above the 1976-2005 averages. The CH_4 diffusion parameterization was transferable between the four lakes; however, different ebullition parameterizations were required for the two deeper lakes (~6-7 m mean depth) versus the two shallower lakes (~1-3 m mean depth). Relative to using observed meteorological forcing, which had a cold bias (-0.15 to -0.63 °C) and RMSE of 0.38 to 0.90 °C, the GCM-forced models had a warm bias (+0.96 to +3.13°C) and marginally higher RMSE (1.03 to 3.50°C) compared to observations. The results support continued efforts to couple CH_4 lake-emission models to GCMs without downscaling meteorological data, allowing feedback between CH_4 dynamics and future climates to be modelled.

Plain Language Summary

Climate change in the Arctic is moving at a greater rate than in the rest of the world. The urgency of characterizing greenhouse gas emissions from water bodies in high latitudes has become a subject of intensive research during the last two decades. It is believed that methane (CH4) emissions from freshwater systems are the most important source of uncertainty in the global greenhouse gas budget, and their contribution has been excluded from earth systems models.

Previous models have been developed to determine these emissions; however, they often require several inputs and lake characteristics that are not readily available. Considering this, we developed a subroutine to determine CH4 fluxes and concentrations in the water column for four lakes located in Arctic Alaska. Subsequently, we implemented meteorological data from a climate model to predict future CH4 fluxes. The calculated increases in atmospheric fluxes were significant; emissions from all the studied lakes are expected to increase at least 38% over the next 80 years. Our study presents a simple formulation with limited constraints to estimate CH4 emissions. We expect that our subroutine could be embedded into climate models to predict emissions from the Arctic and potentially from the rest of the globe.

1 Introduction

Atmospheric CH_4 emissions from lakes form a large portion of the global greenhouse gas (GHG) budget (10-16%; Bastviken et al., 2011), with lake sediments being a reservoir for mineral and organic carbon, which is released as CH_4 (as well as CO_2; Dean and Gorham, 1998; Zhang et al., 2017). CH_4 emissions from lakes vary with seasonal changes in temperature and these fluctuations are primary drivers of intra-annual variation in global CH_4 emissions (Greene et al., 2014; Wik, Varner, and Walter Anthony, et al., 2016). Under the RCP 2.6 emission scenario from 2080 – 2100, higher lake surface water temperatures and longer ice-free seasons are expected globally (2.5°C and 15 days, respectively; Woolway and Merchant 2019); with warming 2-3 times more severe in the Arctic (Graversen et al., 2008; Belkin, 2009; Bintanja, 2018).

Rapid Arctic warming will increase CH_4 emissions by thawing permafrost, but will also increase the rate of CH_4 release from lakes through enhanced microbial decomposition in the sediments (Walter Anthony and Anthony, 2013). Higher temperatures will also decrease the duration of ice cover, which is relevant as ice promotes dissolution of CH_4 bubbles into the water column, and subsequent accumulation under ice (Denfeld et al., 2018). A shorter duration of ice cover will result in increased ebullition and diffusion; although increased oxidation is also expected, enhanced CH_4 productivity may exceed this loss (Greene et al., 2014; Martinez-Cruz et al., 2015).

The increased ebullitive and diffusive CH_4 fluxes, from temperature-driven enhancement of productivity in anoxic sediments (Zeikus and Winfrey, 1976; Walter Anthony et al., 2006; Zhang et al., 2017), suggests a positive feedback loop, because model projections of future climate change depend strongly on the atmospheric concentration of GHGs (Harriss et al., 1993; Whalen, 2005). Small lakes are presently not resolved in climate models (MacKay et al., 2009), and so there is a need to include this positive feedback from Arctic lake systems into climate model land surface schemes.

Correspondingly, efforts have been made to incorporate emissions from freshwater systems into regional and global GHG budgets. Observations from individual lakes have been up-scaled according to lake-size distributions (Bastviken, Ejlertsson and Tranvik, 2002; Bastviken et al., 2004; Wik, Varner and Walter Anthony, et al., 2016; DelSontro, Beaulieu and Downing, 2018). Process-based models have also been developed to simulate CH_4 dynamics in freshwater systems (Tan, Zhuang and Walter Anthony, 2015; Stepanenko et al., 2016); however, they require lake characteristics and calibration variables that are not typically measured.

Tan and Zhuang (2015) coupled a lake model to downscaled output from a climate model (one-way coupling) to project present and future CH_4 emissions from Arctic lakes. Their results showed that the emissions will roughly double by the end of the 21st century. However, because of the bias-correction and interpolation applied in their downscaling, their models are not able to be run as part of a climate model land surface scheme that would enable positive feedback between CH_4 emissions and increased future temperatures.

The purpose of the present study is to develop a scalable CH_4 emission model (Hurtado Caicedo, 2019) that may be coupled to the one-dimensional (1D) Canadian Small Lake Model (CSLM;

MacKay 2012, MacKay et al., 2017). Although not part of the present study, these models can be embedded in the land surface scheme (CLASS) of the Canadian Regional Climate Model (CRCM; Verseghy and MacKay, 2017) and hence would be able to capture the feedback between CH_4 emissions and climate change. The specific objectives are to (1) assess the ability of the CSLM-CH_4 model to estimate present water temperatures and CH_4 emissions, from four Arctic lakes, without downscaling the CRCM output used as surface forcing; and (2) project future CH_4 emissions under various GHG emission scenarios for the four Arctic lakes.

2 Methods

2.1 Study sites

Four Arctic kettle lakes near Toolik Field Station (68°38′ N, 149°39′ W) were modelled: Toolik Lake and Lakes E1, E5 and E6 (Figures 1, S1 and S2). The lakes are located in the continuous permafrost zone on the North Slope of Alaska in the Brooks Range foothills region. These water bodies are part of the Arctic Long-Term Ecological Research (ARC LTER) program and have been widely studied in order to understand the impact of environmental change on their physical and chemical properties (O'Brien, 1992; MacIntyre et al., 2006; Walter Anthony et al., 2008; Jorgenson et al., 2010; Hobbie and Kling, 2014).

Lakes characteristics (surface area, bathymetry and extinction coefficients) were available from MacIntyre et al. (2018; Table 1). Given the predominantly flat-bottomed bowl shape of kettle lakes (Fig. S1), simulations resolved from the free surface to the mean ($\mathbf{Z_{mean}}$), as opposed to the maximum ($\mathbf{Z_{max}}$) lake depth (see MacKay, 2012).

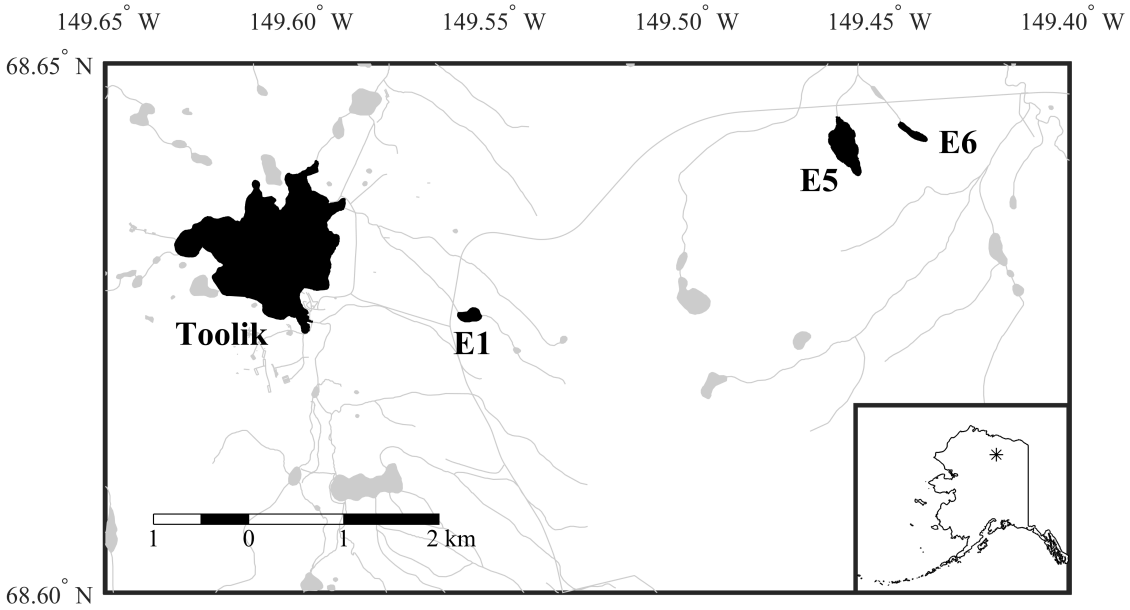

Figure 1. Map of Alaskan Artic lakes simulated in this study: Toolik Lake and three smaller, nearby lakes E1, E5 and E6.

2.2 Forcing and validation data

2.2.1 Observed meteorological forcing

Meteorological data was collected by Kling (2000) at the surface of Toolik Lake during the ice-free seasons (June - September) of 2001-2005. Incident shortwave and longwave radiation were measured with a Kipp and Zonen CM3 radiation sensor at ~50 cm height above the lake surface. Air temperature and relative humidity were measured with Vaisala HMP45C (2.5-3 m above the water surface), and wind speed was measured with a Met One 014A anemometer (3.8-5 m above the water surface, Table 2) and corrected to 10-m using a logarithmic model (Holmes, 2001). Given their proximity (Figure 1), the same meteorological forcing was applied to all four lakes.

2.2.2 Modelled meteorological forcing

Baseline (1976-2005) and future (2071-2100) global climate model (GCM) forcing data were obtained from the simulations of the Canadian Earth System Model (CanESM2/CGCM4), which was run as part of CMIP5 with a 50-km grid resolution. The emission scenarios included the Representative Concentration Pathways 2.6 (RCP 2.6), 4.5 (RCP 4.5) and 8.5 (RCP 8.5). RCP 2.6 is a low greenhouse gas emission scenario in which changes to the radiative forcing would lead to an increase in the global mean temperature of 1°C. Under RCP 2.6, global carbon emissions are projected to decrease to near zero by the end of 2100. Under the medium emissions scenario, RCP 4.5, changes to the radiative forcing cause a 2°C increase in air temperature under stabilized GHG emissions, and under the high emission scenario RCP 8.5, changes to the radiative forcing result in an increase of 3.7°C in air temperature with a continuous growth of GHG emissions (IPCC, 2013).

2.2.3 Observed temperature time series

Water temperature time-series at Toolik Lake and Lakes E5 and E6 were collected by S. MacIntyre (ARC LTER; https://arc-lter.ecosystems.mbl.edu) during the summers of 2001-2005. Water temperature was measured with moored, self-contained loggers (see Table S1 for logger depths). In Toolik Lake RBR Ltd. TR-1050s (±0.002°C) and in Lakes E5 and E6, StowAway Tidbit Loggers (±0.21°C) were used.

2.2.4 Observed CH_4 fluxes

CH_4 ebullitive fluxes from Toolik Lake in 2004 were digitally retrieved from Tan et al., (2015; their Figure 10). They collected gas samples using submerged bubble traps over ebullition seeps along defined transects in the lake from April 28, 2003 to December 31, 2004. Subsequently, lake-wide daily ebullition was determined as the sum of the fluxes from each seep type and averaged over the lake surface area.

Continuous diffusion and ebullition data for lakes E1, E5 and E6 were not available; however, aggregate values of seasonal and mean annual fluxes were used as given in Sepulveda-Jauregui et al. (2015). They determined the mean annual fluxes as the sum of different modes of emission in the summer (ice-free season), winter and spring. Sepulveda-Jauregui et al. (2015) performed measurements from June to July (2011–2012) and extrapolated the value to the entire ice-free season. They calculated ebullitive fluxes by multiplying the average seep densities on each lake by the sum of daily ebullition from seeps of each type. We compared our simulated surface

diffusive fluxes from Toolik Lake during the summer seasons of 2010–2015 to measurements by Eugster et al. (2020a), who deployed a three-dimensional ultrasonic anemometer–thermometer and a closed-path integrated off-axis cavity output spectrometer.

Table 1. Lake characteristics. Z_{max} and Z_{mean} are maximum and mean lake depths respectively, and k_d is the extinction coefficient (MacIntyre, Cortés and Sadro, 2018).

	Latitude (°N)	**Longitude (°W)**	**Area (km^2)**	**Z_{max} (m)**	**Z_{mean} (m)**	**k_d (m^{-1})**
Toolik Lake	68.633	-149.607	1.49	26.0	7.4	0.6
Lake E1	68.626	-149.555	0.029	12.0	3.1	0.8
Lake E5	68.642	-149.458	0.109	12.9	6.4	1.1
Lake E6	68.643	-149.441	0.019	3.0	1.6	1.4

Table 2. Calibration parameters for each lake. The wind sensor height and hypolimnion turbulent diffusivity were adjusted, on a lake-by-lake basis, to account for sub-grid-scale turbulent mixing and for spatial variability in wind speed and surface drag (which is computed internally in the model). $\mathbf{C_{labile}}$ and $\mathbf{k_{ox}}$were adjusted to minimize CH_4 RMSE.

	Wind sensor height (m)	**C_{labile} (mg m^{-2})**	**Hypolimnion turbulent diffusivity, K_Z (m^2 s^{-1})**	**CH4 oxidation k_{ox} (s^{-1})**
	(A)	(B)	(C)	(D)
Range	3.8 – 10	90 – 280	10^{-5} – 10^{-9}	10^{-5}-10^{-8}
Toolik Lake	3.8	280	10^{-7}	1.74×10^{-5}
Lake E1	5.0	280	10^{-7}	1.74×10^{-5}
Lake E5	5.0	280	10^{-7}	1.74×10^{-5}
Lake E6	3.8	280	10^{-7}	1.74×10^{-5}

2.2.5 Observed CH_4 concentrations

CH_4 concentration profiles were measured in Toolik Lake and lakes E1, E5 and E6 during the ice-free seasons of 2013-2016 by MacIntyre and Cortés (2017). CH_4 was measured using the headspace equilibrium method and gas chromatography. A summary of the collected data and sources specified in section 2.2 is presented in Table S2.

2.3 Modelling framework

Climate models are typically validated against long-term averages (e.g., climate normals); however, they also show skill in reproducing characteristic large-scale distributions of air temperature, precipitation, radiation and wind. For example, the dynamics of monsoon systems, seasonal temperature changes and storm tracks. Climate models can even predict weather over seasonal timescales and capture interannual variability (Randall et al. 2007). As a result, output from climate models is frequently applied to drive lake models to forecast the impacts of climate change on lake hydrodynamics and water quality (e.g., Woolway et al. 2020; Bolkhari et al. 2022; Golub et al. 2022). When run as hindcasts, it is expected that these GCM-forced models will reasonably capture observed variation in meteorological conditions over seasonal to inter-annual timescales.

To evaluate forcing-bias when developing coupled lake-atmosphere models, it is a requirement to test the accuracy of the lake model when forced directly with atmospheric (or climate) model output, in comparison to being forced with observed meteorological forcing (e.g., Huang et al. 2010). Consequently, simulation dates were selected based on the availability of both meteorological forcing data sets (observations and GCM model output) and water temperature calibration data (ARC LTER). Three different calibration scenarios were run: (1) with observed meteorological forcing for the ice-free season of individual years (Toolik Lake: 2001-2005; Lake E5: 2002-2005; Lake E6: 2003-2005; no lake temperature data was available for Lake E1); (2) with GCM-generated meteorological data for the ice-free season of individual years; and (3) with GCM-generated meteorological data in a continuous 'baseline' run from 1976-2005. Simulations (1) and (2) were to assess the error in applying GCM forcing without downscaling; simulation (3) was to test for long-term model drift.

The GCM output is a statistical representation of the atmospheric conditions in each year, and thus does not necessarily capture the exact timing of particular meteorological events (e.g., the passage of a cold front; Figures S4-S6). Therefore, here we quantitatively compared mean seasonal observed temperature profiles, as opposed to conventional contours of temperature time-series with depth. The latter type of comparisons is given in Hurtado Caicedo (2019) and Figure S7.

Temperature profiles for model initial conditions were not available from ARC LTER in 1976; therefore, Toolik was initialized with historic data (Giblin and Kling, 2015), while E5 and E6 used initial profiles from 2002 and 2003, respectively. For simulations with future GCM data (2071-2100), initial water temperatures were from observations in 2013. Initial CH_4 profiles were as reported by MacIntyre and Cortés (2017). For long-term simulations, it is expected that the model will lose knowledge of the initial conditions within the first year of simulation (1977 for the baseline run and 2072 for the future simulations; Figure S3), hence model results during this time were disregarded.

2.3.1 Model description

The approach to determine CH_4 emissions consisted of two parts: (1) implementation of a pre-existing thermodynamic lake-tile model to calculate the surface mixed layer depth and unsteady temperature profile through the water column, and (2) the development of a new CH_4 subroutine to compute CH_4 ebullition, dissolved CH_4 flux from the sediments, diffusive CH_4 flux below the surface mixed layer and through the air-water interface.

Temperature: Temperature profiles were simulated using the 1D (vertical) thermodynamic CSLM lake-tile model, which incorporates a bulk mixed-layer turbulent kinetic energy budget to simulate a 1 m^2 water column, characteristic of a lake with a specified surface area, mean depth and light extinction coefficient (Table 1; MacKay, 2012; MacKay et al., 2017). We acknowledge that a mean depth approach underestimates water temperature in the littoral zone and overestimates water temperature at depth. We justify this by noting that the resulting lower modelled fluxes in shallow zones and higher modelled fluxes at depth will partially cancel and that the objective here is to develop a feasible lake-tile CH_4 model and not to simulate CH_4 fluxes as accurately as possible. The hypolimnion turbulent diffusivity K_z and wind sensor height were adjusted, on a lake-by-lake basis (Table 2), to account for variation in sub-grid-scale turbulent mixing and for spatial variability in wind speed and surface drag (which is computed internally in the model).

The model had $\Delta z = 0.5$ m vertical grid resolution and used 5 or 15-minute timesteps (Δt) when forced with observed and GCM-derived meteorological data, respectively. Ice cover was modelled according to the snowpack physics module of CLASS, which was shown to reproduce ice-on/off dates to within 1 week of observations in Lake 239 (MacKay et al. 2017).

CH_4 ebullition: To model CH_4 emissions within a land-surface scheme, model parameterizations must be a function of variables readily obtained from GCM output, which limits model complexity. We parameterize CH_4 ebullition for the deeper ($\mathbf{Z_{mean}}$ = ~6-7 m; Toolik and E5) and shallower ($\mathbf{Z_{mean}}$ = ~1-3 m; E1, E6) lakes according to Eq. 1 and 2, respectively, which are empirical temperature-dependent functions (Wik et al., 2013, 2014; Wik, 2016, Aben et al., 2017):

$$\boldsymbol{E = -0.00036T^3 + 0.16T^2 - 0.94T + 1.48} \quad (1)$$

$$\boldsymbol{E = 141 \times 1.19^{(T-20)}} \quad (2)$$

The above expressions correlate the average ebullitive flux E (mg CH_4 m^{-2} d^{-1}) to the average sediment surface temperature T (°C); assumed to be the modelled bottom water temperature. CSLM is a water column model, that does not account for the distribution of sediment surface area with lake depth. The model does not resolve littoral sediments, with higher temperatures that contribute more ebullitive flux during summer (Bastviken et al., 2004; Wik, Varner, and Walter Anthony, et al., 2016). To account for this, we use mean depth hypsometry and depth-based parameterizations for the shallower (E1 and E6; Eq. 2) and deeper (Toolik and E5; Eq. 1) lakes.

The parameterization in Eq. 1 was from 6806 ebullitive flux observations in three sub-Arctic lakes in northern Sweden (68°21′ N, 19°02′ E) during the ice-free seasons (June–September) of

2009-2014 (Wik et al., 2013, 2014; Wik, 2016). The parameterization in Eq. 2 (Fig. 1 and equation 2 in Aben et al., 2017) was developed for shallower Boreal ponds based on measurements by DelSontro et al. (2016), including 77 observations during the ice-free season (May–October of 2011, 2012 and 2014) from ten shallow ponds located in the Saguenay region of Quebec (48°23'N, 71°25' W), and 83 observations from three lakes in the Laurentian region of Quebec (45°59' N 73°89' W).

Our attempts using Eq. 1 to determine ebullitive fluxes for the shallower lakes resulted in underestimation of emissions in comparison to observations; likely because we do not explicitly resolve littoral sediments. These values were similar in order of magnitude to the results obtained for Toolik Lake. Shallower systems (ponds < ~3 m depth) have been shown to have CH_4 fluxes ~10 times greater than deeper systems (lakes ~3-30 m depth), supporting our usage of a different parameterization for ponds versus lakes (Wik, Varner and Walter Anthony, et al. 2016). For instance, ebullitive fluxes from the shallower systems can be up to ~9 times greater than those from the deeper systems (see Table S3). The other equations in Aben et al., (2017) were also evaluated (not shown) but performed worse than Eq. 1 and 2.

Dissolution of rising bubbles was neglected because of the shallow lake depths (Schmid et al. 2007). The present model also does not inhibit ebullition through ice during winter. Ebullition would be stored within the ice (Walter Anthony et al., 2008; Walter Anthony et al., 2006) and subsequently released during break-up (Phelps, Peterson and Jeffries, 1998a; Juutinen et al., 2009; Karlsson et al., 2013). Consequently, methanotrophy (oxidation) of dissolved CH_4 from rising bubbles was also neglected, since previous work suggests that for systems < 20 m deep, less than 10% of the CH_4 is lost due to dissolution during rise (McGinnis et al., 2006; Schmid et al., 2007). These limitations will be addressed in future work.

Dissolved CH_4 and diffusive sediment flux of CH_4: The CH_4 profile in the water column was simulated by numerically solving the 1D diffusion equation (Eq. 3) with terms for turbulent diffusivity, oxidation and production at the sediment-water interface (e.g., Schmid et al., 2007; Jabbari et al., 2016):

$$\frac{\partial C_{CH_4}}{\partial t} = \frac{\partial}{\partial z}\left(K_z \frac{\partial C_{CH_4}}{\partial z}\right) - k_{Ox}\left(C_{CH_4}\right) + P \tag{3}$$

Here, C_{CH_4} (mg L^{-1}) is the CH_4 concentration, K_Z (m^2 s^{-1}) is the vertical turbulent diffusivity below the surface mixed layer (Table 2; ~10^{-7} m^2 s^{-1}; Nakhaei et al. 2016), k_{Ox} (s^{-1}) is the first-order CH_4 oxidation rate coefficient (1.74×10^{-5} s^{-1}; Thottathil et al., 2019), P (mg CH_4 m^{-3} d^{-1}) is the production term (Eq. 4), t is time and z is the vertical coordinate direction. We acknowledge that K_Z, in these relatively shallow lakes, is likely orders of magnitude larger than this near-molecular value; however, the turbulent diffusivity and/or dissipation in a calibrated sub-grid-scale closure scheme is often not equal to observed values (Boegman et al., 2021; Lin et al., 2022).

Our first-order oxidation model was developed following Schmid et al. (2007). From a sensitivity analysis (10^{-5} s^{-1} < k_{Ox} < 10^{-8} s^{-1}), we selected the observed value k_{Ox} ~ 1.74×10^{-5} s^{-1} by Thottathil et al. (2019) from 6 lakes in Quebec (Canadian Shield). For a CH_4 concentration of

305 C_{CH_4} ~ 0.1 μmol L^{-1} (Figs S8-S11), the resulting oxidation was consistent with observed rates
306 (~10^{-6} to ~10^{-5} μmol L^{-1} s^{-1}) from shallow Alaskan lakes (Lofton et al. 2014).

307 The oxidation term was applied throughout the water column and the turbulent diffusion term
308 was applied to drive CH_4 flux from the base of the surface mixed layer to the bottom cell. CH_4
309 production from sediments P (mg m^{-2} s^{-1}) was applied as a flux into the cell above the sediment-
310 water interface (Tan et al. 2015):

$$\boldsymbol{P = R_C C_{labile} PQ_{10}^{\left(\frac{T-T_{pr}}{10}\right)}} \quad (4)$$

311 where R_C (0.02 s^{-1}) is the fraction of carbon converted per year, PQ_{10} (3.5) is the factor by which
312 production increases with a 10°C rise in temperature, T_{pr} is the reference temperature for CH_4
313 production, which is approximately equal to the yearly mean sediment temperature below the
314 water column (-3.0 °C) and T (°C) is the sediment surface temperature (Tan et al., 2015);
315 assumed to equal the modelled bottom water temperature at the mean depth. Here, C_{labile} (mg m^{-2})
316 is the areal labile carbon density. To directly model the carbon pool requires soil incubation
317 data and knowledge of the thickness of the talik layer (Tan et al., 2015). Unlike the lake-specific
318 parameters in Table 1, these parameters are not known across the CRCM domain; therefore, we
319 estimated C_{labile} = 280 mg m^{-2} (Table 2), by minimizing the difference between the observed and
320 modelled CH_4 concentrations in the water column. Ideally, for the model to be scalable, C_{labile}
321 will be the same for all lakes or a function of the lake-specific parameters in Table 1. This
322 approach is not new, and it what is typically done to set the sediment oxygen demand in
323 biogeochemical lake models (e.g., Scalo, Boegman and Piomelli, 2013).

324 With Eq. 4, the model may account for both the ^{14}C-enriched carbon pool from the upper
325 sediment layer constituted by newly settled organic matter, since both Toolik Lake and Lake E5
326 are considered nonyedoma/nonthermokarst lakes (Stepanenko et al., 2011, 2016; Sepulveda-
327 Jauregui et al., 2015; Tan and Zhuang, 2015). According to Tan, Zhuang and Walter Anthony
328 (2015), CH_4 in nonyedoma lakes is mainly produced in surface sediments from newly deposited
329 ^{14}C-enriched organic matter.

330 The constants R_C,PQ_{10} and T_{pr} were as specified by Zhuang et al. (2004) for the alpine tundra
331 and polar desert ecosystem of the Toolik area. To account for productivity in the upper sediment
332 layers (Peeters, Encinas Fernandez and Hofmann, 2019), and based on the shallow bowl-like
333 bathymetry of the smaller lakes (Fig. S1 and S2), P was added fractionally at each depth of water
334 (Schwefel et al., 2018); this was accomplished by calculating P and dividing the result by the
335 number of layers in the water column (14, 13, 6 and 4 layers for Toolik, E5, E1 and E6
336 respectively).

337 *Diffusive flux of CH_4 to the atmosphere.* The rate of CH_4 transfer across the water-air interface
338 was specified following Happell et al. (1995) and Schmid et al. (2007):

$$\boldsymbol{F_{CH_4} = f(W) K_{ex} (C_W - C_A)} \quad (5)$$

where K_{ex} (m s^{-1}) is the gas transfer velocity (O'Connor, 1983), f(W) is a coefficient that determines the influence of wind speed (equal to $1 + 0.058W^2$ for $W \leq 5$ m s^{-1} and $1 + 0.047W^2$ for $W \geq 5$ m s^{-1}; Schmid et al., 2007), C_w (mg L^{-1}) is the modelled CH_4 concentration at the water surface and C_A (mg L^{-1}) is the atmospheric equilibrium CH_4 concentration (Wiesenburg and Guinasso, 1979), which is a function of the surface temperature and the measured atmospheric CH_4 concentration (1700 ppb from 1976–2005 and projected to be on average 1300, 1600 and 3600 ppb under RCP scenarios 2.6, 4.5 and 8.5, respectively, from 2071–2100; Meinshausen et al., 2011). The diffusive CH_4 flux to the atmosphere was restricted during ice-cover period and the accumulated gas was subsequently released into the atmosphere at ice-off.

2.4 Flux aggregation

The model computed CH_4 ebullitive and diffusive fluxes at 5 min intervals, when forced with observed meteorological data, and 15 min intervals, when forced with GCM-generated data. Mean daily and mean annual fluxes were averages of these outputs over each day or year. Total surface fluxes refer to the sum of ebullitive and diffusive fluxes. These were compared to observed ebullitive and diffusive fluxes collected as described in section 2.2.4. We acknowledge that spatial and temporal extrapolation of the observations may introduce error (e.g., they neglect background non-seep emissions); however, these were the best available data (Sepulveda-Jauregui et al. 2015) and followed well-established practices (Bastviken et al. 2011). For Toolik Lake, daily ebullitive fluxes from point source seeps in the lake centre, were digitally retrieved from (Tan et al., 2015), averaged over July 4 to August 18, 2004 and compared to the modelled average over the same period.

3 Results

3.1 Model calibration (observed meteorological forcing)

The coupled CSLM-CH_4 model (Hurtado Caicedo, 2019) was developed and calibrated for all four lakes over a 3 to 4-year duration simulation (Figures S8-S11) using the observed meteorological data. Simulated temperature profiles had depth-dependent root-mean-square errors (RMSE) <3.2 °C, which were highest through the thermocline, where small differences in the simulated thermocline depth can lead to larger RMSE (e.g., Boegman and Sleep, 2012). These were in the range of literature values, from large lake model applications (3 < RMSE < 7 ºC; Huang et al., 2010; Paturi et al., 2012) and other pond simulations (RMSE < 3.03 ºC; Nakhaei et al., 2018). The surface RMSE <1.5 °C was less than 1.96 ºC for other small boreal lake simulations (Stepanenko et al., 2016) and comparable to 1.5 ºC from other Arctic lake simulations (Tan et al., 2015).

The dissolved CH_4 concentrations were <0.6 μM (Figures S8-S10), which is reasonable in comparison to errors from more complex CH_4 models (Stepanenko et al., 2011, 2016; Tan et al., 2015). The RMSE for Lakes E1 (< 0.2 μM), E5 (< 0.05 μM) and Toolik Lake (< 0.03 μM) were consistent with the mean errors found by Tan et al., (2015) and Stepanenko et al. (2016), which ranged from 0.01 μM to 0.26 μM. However, the RMSE for Lake E6 were larger, ranging from 0.3μM to 0.6 μM.

The simulated mean-daily summer ebullitive fluxes from Toolik Lake in 2004 were within 2% of measured values (7.04 vs. 6.91 g m^{-2} d^{-1}, respectively: Table S3). Although ebullition

observations were not available for the other lakes (E1, E5 and E6) during the same years as observed meteorological forcing (2013-16), observed ebullition data from 2011-12 were included for comparison (Table S3). The simulated mean summer fluxes were 19% (9.53 mg CH_4 m^{-2} d^{-1}), 21% (0.72 mg CH_4 m^{-2} d^{-1}) and 30% (25.74 mg CH_4 m^{-2} d^{-1}) lower than observed in E1, E5 and E6 over 2011-12.

The simulated mean-daily summer surface diffusive fluxes from Toolik Lake in 2015 and 2013 were within 20% of measured values by Eugster et al. (2020a; Table S4). As with the observed ebullitive fluxes, observed diffusive fluxes were not available for lakes E1, E5 and E6 during 2014–2015, and so were compared to observed data from other years. For lakes E5 and E1, the observed fluxes were larger than simulated value, whereas for E6 the simulated flux was larger (Table S4). These data should be interpreted with caution, as the 2012 diffusive surface flux observed by Sepulveda-Jauregui et al. (2015) from Toolik Lake is ~3 times larger than the value observed by Eugster et al. (2020a). Therefore, values reported by Sepulveda-Jauregui et al. (2015) for the shallower systems may also be overestimated.

3.2 Hindcast simulations (1976-2005 GCM forcing)

Simulated temperatures: Simulations forced with GCM data, initialized in individual years, were better in comparison to observations, relative to the long-term GCM-forced simulations (Figure 2); except Toolik (in 2001) and E5 (in 2003 and 2004). The GCM-forced model had a systematic shift to higher temperatures in some years (≤ ~4 °C in Toolik, Fig. 2d; ~5 °C in E5), where the seasonal thermocline intersected the lakebed. The shallower Lake E6, had more satisfactory results (<2 °C bias). The temperature overestimation, simulated with the GCM, resulted from higher incident longwave radiation in the GCM compared to the observed data (23 W m^{-2} higher on average; Table S5), warmer air temperatures (1 °C higher on average, with exception of 2005) and higher wind speeds (1.5 m s^{-1} higher on average; Table S5). The GCM-forcing causes higher temperatures and deepening of the thermocline relative to observations, and thus higher sediment temperatures when the thermocline approaches the lakebed (mean depth).

In 2004, there was observed temperature data (Toolik, E5 and E6), as well as forcing for all three simulations (forced with observed 2004 meteorology, forced with 2004 GCM meteorology and forced with 1976-2005 GCM meteorology). Intercomparison of performance metrics (Table 3) show RMSE (0.38 to 0.87 °C vs. 1.03 to 3.50 °C) and NRMSE (0.03 to 0.08 vs. 0.07 to 0.30) to be marginally less for observed forcing, compared to GCM forcing. The observed and GCM forced simulations had cold (+0.01 to -0.63 °C) and warm (+0.96 to +3.13°C) biases, respectively. The high R^2 (0.99 for observed forcing and 0.74-0.99 for GCM forcing) indicates that the observed temperatures are explained by the models. In 2004, the GCM underestimated observed shortwave radiation by 9.3%, overestimated longwave radiation by 6.4% and air temperature by 4.6% (Table S5). However, it remains difficult to generalize this error as GCM biases are different from year to year (Table S5). There was no discernable difference in metrics for the 2004 GCM vs. 1976-2005 GCM forcing, indicating that long-term model drift was not an obvious source of error.

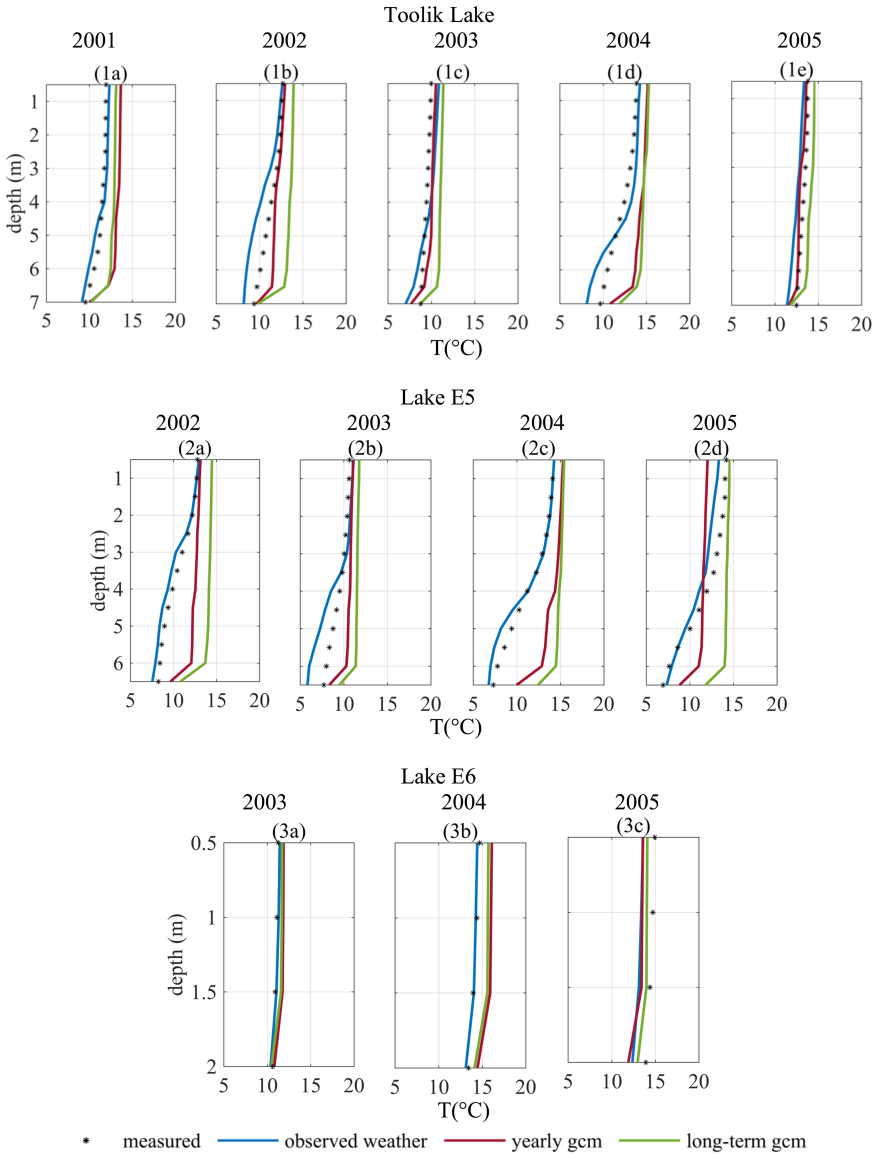

Figure 2. Comparison of measured time-averaged water temperature with simulations. Black stars are measured temperature, blue lines show the simulations with observed meteorological data, red lines show simulations with GCM data and initial conditions at the beginning of the simulation period for each year, and green lines show simulations with GCM data starting in 1976. Temperature validation were from Jul. 16 to Aug. 11 in 2001, Jul. 2 to Aug. 10 in 2002 and Jun. 28 to Aug. 18 in 2004.

Simulated CH_4 fluxes: The baseline (1976-2005) average annual surface flux (sum of ebullition and diffusion; Table 4A) was compared to the average total annual 2011-2012 emission observations reported by Sepulveda-Jauregui et al. (2015). The simulated baseline fluxes for the shallower lakes (Table 4A; from 8.43 ± 3.72 g CH_4 m^{-2} yr^{-1} in E1 to 8.65 ± 4.01 g CH_4 m^{-2} yr^{-1} in E6) were within 34% of the observations (Table 4B; from 9.4 g CH_4 m^{-2} yr^{-1} in E1 to 13.3 g CH_4 m^{-2} yr^{-1} in E6).The observed total fluxes were higher in Lake E6 than in Lake E1, which was captured by our model (Table 4). For the shallower lakes, the modelled surface fluxes were

smaller than observed fluxes, which could result from Sepulveda-Jauregui et al. (2015) extrapolating emissions from June-July observations, when sediment temperatures were much higher, to the entire ice-free season (considered to be May-September) and therefore likely overestimating fluxes (Section 3.1).

The modelled baseline fluxes for the deeper lakes (Table 4A; from 3.79 ± 1.54 g CH_4 m^{-2} yr^{-1} in Toolik to 4.20 ± 1.52 g CH_4 m^{-2} yr^{-1} in E5) were larger than the observations from Sepulveda-Jauregui et al. (2015), for 2011-2012 (Table 4B; from 2.0 g CH_4 m^{-2} yr^{-1} in Toolik to 1.4 g CH_4 m^{-2} yr^{-1} in E6). This discrepancy can be attributed to the warm bias of the GCM forced models, which was more prominent in the deeper systems (Table 3; Figure 2).

3.3 Forecast simulations (2071-2100 GCM forcing)

Air temperature. Under RCP scenarios 2.6, 4.5 and 8.5, the air temperature in the Toolik Lake area was modelled to increase 3.6–7.3°C (Figure 3; Table 6) over the next 80 years. This is consistent with the rates that have been reported for the entire Arctic over the past century (Graversen et al., 2008; Belkin, 2009; Bintanja, 2018). RCP 8.5 shows a strong and continuous increase in air temperature, which is more abrupt than under baseline conditions, RCP 4.5 has a consistently increasing trend and RCP 2.6 shows a decline in air temperature over 2071-2100.

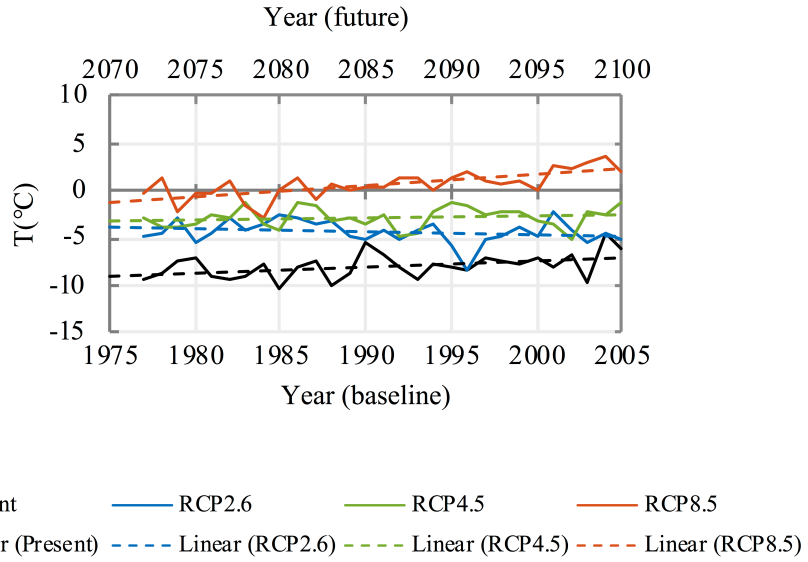

Figure 3. Comparison of baseline and future simulations of average yearly air temperature. Baseline data correspond to GCM data in years 1976 – 2005 (black line) and future data correspond to GCM data in years 2071 – 2100 under RCPs, 2.6 (blue line), 4.5 (green line) and 8.5 (red line).

Bottom lake temperature. The simulated increases in bottom-water temperature (from 1976-2005 to 2071–2100) were similar between the lakes (Table 6A; Figure 4 and Figure 5). For RCP 2.6, 4.5 and 8.5, the average bottom temperatures increased 0.61–0.84°C, 0.94–1.21°C and 1.82–2.24°C, respectively, over 2071–2100 relative to the 1976–2005 baseline. Inter-annual variability in average bottom temperature was ~2 °C, with a more pronounced overall increase in bottom lake temperature under RCP 8.5 (Figures 4 and 5).

Sediment CH_4 diffusion. Average diffusive fluxes from the lake sediments over 2071–2100 ranged between 40.24–72.03 mg CH_4 m^{-2} d^{-1} (under all RCPs). Lake E5 had the lowest fluxes of 40.24 – 61.28 mg CH_4 m^{-2} d^{-1} (Table 6 and Figure 4). The shallower lakes E1 and E6 had similar increases in the sediment flux for all scenarios (increasing 8.25 – 27.94 mg CH_4 m^{-2} d^{-1} or 19–63% from 1976-2005 to 2071-2100, Table 6B). These were larger than those of the deeper lakes (increasing 5.62–21.03 mg CH_4 m^{-2} d^{-1} or 14–52%, Table 6B; Figures 4 and 5) and may be associated with increased sediment warming (Table 6A).

CH_4 ebullitive flux. The simulated CH_4 ebullitive flux was most sensitive to the increases in lake water temperature (Table 6C; Figures 4 and 5), with future fluxes more than doubling over the baseline emissions under the high emission RCP 8.5 scenario in the deeper systems (increasing 3.57-3.67 mg CH_4 m^{-2} d^{-1} or 208–217%, Table 6B, Figure 4). In the shallower lakes, the higher ebullitive fluxes had a smaller percentage change (115–118%), but larger absolute change (12.59–13.12 mg CH_4 m^{-2} d^{-1}, Table 6B), due to Eq. 2 being more sensitive to changes in ebullition with temperature changes (Table 6A). This confirms the more significant impact of climate change on increasing CH_4 ebullition (Aben et al., 2017; Walter et al., 2007; Wik, Varner and Walter Anthony, et al., 2016) relative to increases in diffusion, particularly for shallow systems. Ebullition comprised 15% to 47% of the total CH_4 flux from the four lakes (ebullition plus diffusion under all scenarios), 68% of this total flux was produced by the two shallower lakes (E1 and E6; Table 6C).

Ice-free days. The number of ice-free days increased from 103–111 (1976–2005) to 122–155 (2071–2100) (Table 6E). The number of ice-free days was estimated to be up to 19 days longer under RCP 2.6 and up to 44 days longer under RCP 8.5. The baseline model (1976–2005) estimates were consistent with the mean reported ice-free duration increase for glacial and post-glacial lakes of 20 days (Wik, Varner and Walter Anthony, et al., 2016).

Total surface CH_4 flux. The total flux was modelled to increase by 4.15–4.57 mg CH_4 m^{-2} d^{-1} (40%; RCP 2.6), 6.73–7.74 mg CH_4 m^{-2} d^{-1} (65–67%; RCP 4.5) and 12.79–14.81 mg CH_4 m^{-2} d^{-1} (123–129%; RCP 8.6) for the deeper lakes (Toolik and E5) and 8.66–8.94 mg CH_4 m^{-2} d^{-1} (38%; RCP 2.6), 14.33–14.64 mg CH_4 m^{-2} d^{-1} (62%; RCP 4.5) and 29.24–30.29 CH_4 m^{-2} d^{-1} (127–128%; RCP 8.6) for the shallower lakes (E1 and E6). Tan and Zhuang (2015) estimated similar surface fluxes across the Arctic to increase 87% and 137%, under RCPs 2.6 and 8.5 respectively.

Trends over 2071–2100. The water temperature and CH_4 fluxes increased from the 1976–2005 average to the 2071–2100 average under all RCP scenarios, following the increases in GCM-modelled air temperature. However, this did not always cause increasing trends in the simulated temperature and CH_4 data during 2071–2100. For all lakes, during 2071–2100, RCP 8.5 showed strong increases in bottom water temperature and CH_4 fluxes; RCP 4.5 showed minimal increases in bottom water temperatures (<~1 °C) and flat trends in CH_4 production; and RCP 2.6 showed decreased bottom water temperatures (<~1 °C) and trends of decreased CH_4. This suggests that RCP 2.6 and 4.5 will lead to stabilized Arctic lake temperatures and CH_4 emissions by 2100, at levels 0.61–1.21 °C and 38–67%, respectively, above the 1976–2005 averages.

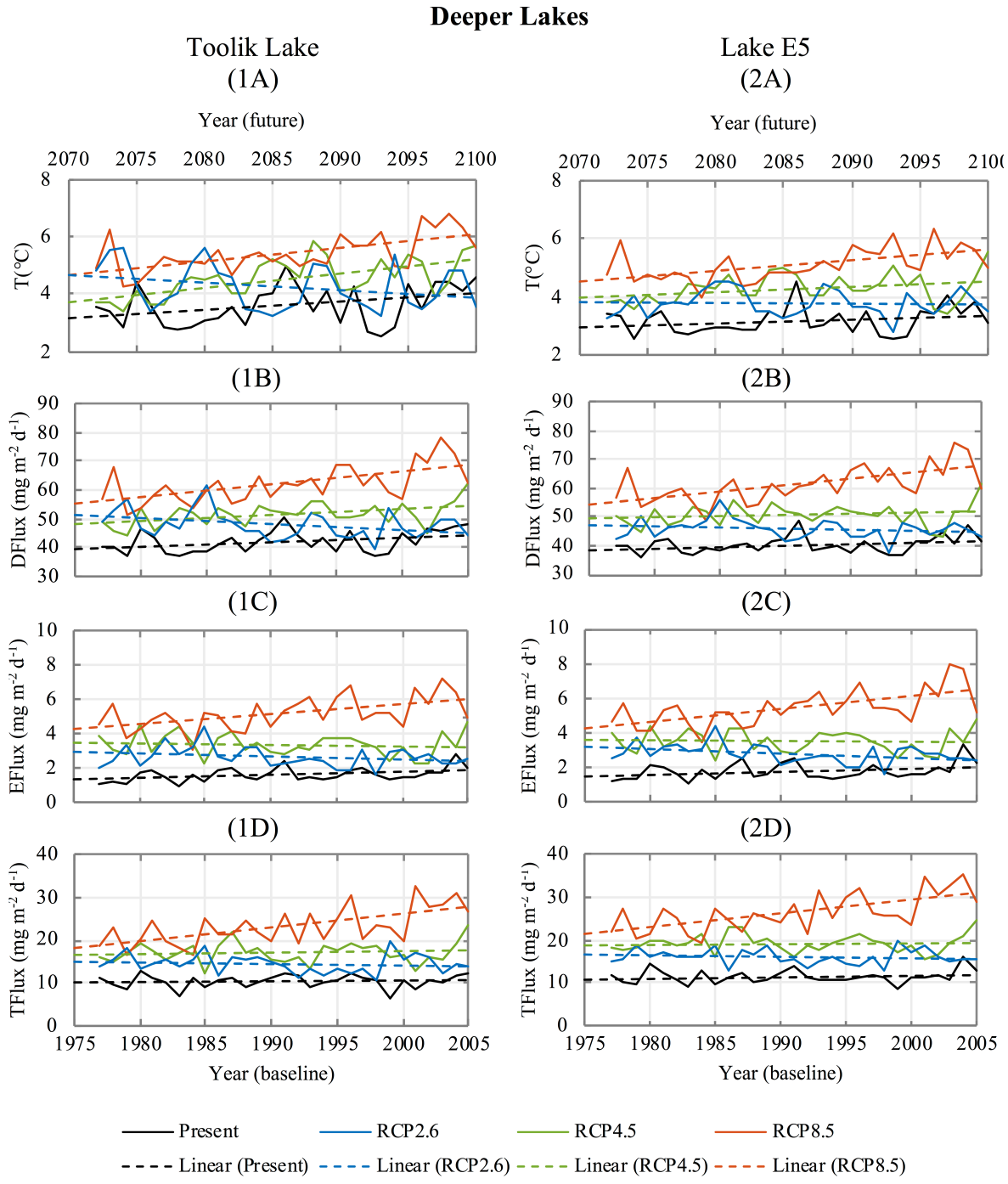

Figure 4. Comparison of baseline and future simulations for the deeper lakes (Toolik and E5; ~6-7 m mean depth), of yearly average A) bottom water temperature B) CH_4 diffusive fluxes at the sediment-water interface C) CH_4 ebullition from sediments and D) total surface CH_4 fluxes.

509

510

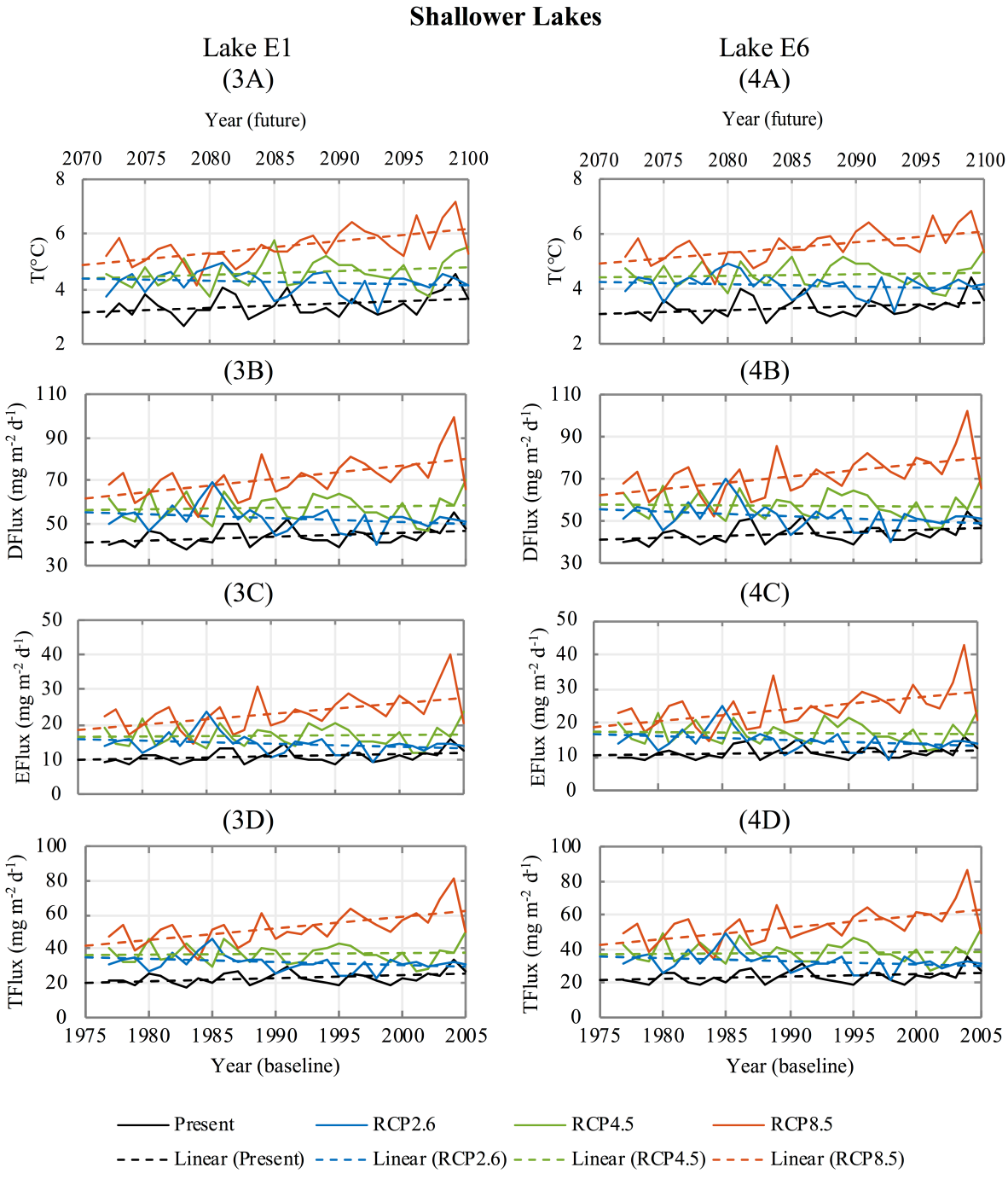

511

512 **Figure 5.** Comparison of baseline and future simulations, for the shallower lakes (E1 and E6; ~1-3 m
513 mean depth), of yearly average A) bottom water temperature B) CH_4 diffusive fluxes at the sediment-
514 water interface C) CH_4 ebullition from sediments and D) total surface CH_4 fluxes.

515

516

Table 3. Statistical metrics comparing (*i*) 2004 simulation forced with observed meteorology, (*ii*) 2004 simulation forced with GCM meteorology and (*iii*) 1976-2005 simulation forced with GCM meteorology to (*iv*) observed temperatures in 2004.This was the only year with observation data and forcing data for all 3 simulations; observed data was not available for Lake E1 in 2004. The GCM data is a statistical representation of the atmosphere and is not expected to reproduce observed meteorology on a day-to-day basis; therefore, before computing the metrics, the higher spatial resolution field observations were interpolated onto the 0.5 m depths of the model grids, then the observed and simulated temperature data were averaged over day-of-year 186 to day-of-year 230, resulting in a single representative mean temperature profile for cases (*i*) to (*iv*). RMSE = root-mean-square error of simulation vs. observation; NRMSE = RMSE/mean(observation); Bias = sum(observation-simulation)/# observations; R^2 = coefficient of determination.

	RMSE (°C)	**NRMSE**	**Bias (°C)**	**R^2**
		Toolik Lake		
Observed 2004	0.90	0.07	-0.15	0.97
GCM 2004	1.98	0.16	+1.86	0.76
GCM 1976-2005	2.39	0.19	+2.28	0.80
		Lake E5		
Observed 2004	0.87	0.08	-0.63	0.99
GCM 2004	2.67	0.23	+2.38	0.81
GCM 1976-2005	3.50	0.30	+3.13	0.77
		Lake E6		
Observed 2004	0.38	0.03	-0.34	0.99
GCM 2004	1.36	0.09	+1.31	0.77
GCM 1976-2005	1.03	0.07	+0.96	0.74

4 Discussion

We have modelled CH_4 emissions from Arctic lakes to increase as a function of increased future air temperature and corresponding increased simulated lake bottom water temperature. In this approach, the following aspects were not included in the model development and may have an impact on simulated future emissions: (1) release of carbon pools contained in permafrost soil as GHGs due to thawing and overall lake/wetland area increase (13% larger, ~0.72 ± 0.19 Mkm^2 under RCP 8.5; Zhang et al. 2017); (2) flux through ice cracks during ice-cover (likely insignificant; Phelps, Peterson, & Jeffries, 1998); (3) contribution of precipitation, which might affect hydrostatic pressure and soil moisture and promote organic matter decomposition by methanogens (Zhang et al., 2017); and (4) inhibition of surface CH_4 ebullition and subsequent storage during ice-cover (Phelps, Peterson and Jeffries, 1998b).

Comparison to previous models. Rather than attempting to improve model precision by downscaling climate model output to be consistent with the re-analysis of weather data (e.g., Tan and Zhuang 2015), we evaluated the implementation of a simple model that may, in theory, be scaled as part of a climate model land surface scheme. This was achieved by using data extracted directly from the GCM, as would be done under two-way coupling.

544
545
546
547 **Table 4.** Summary of simulated mean annual surface fluxes forced with GCM data under baseline (1976-
548 2005) and future scenarios (2071-2100) and observed mean annual surface fluxes from 2011 and 2012
549 (Sepulveda-Jauregui et al., 2015). Percentage change of average value from the baseline value shown in
550 parentheses.
551
552
553

	Total simulated surface flux (g CH_4 m^{-2} yr^{-1})	**Observed total surface flux 2011-2012 from June-July extrapolation (g CH_4 m^{-2} yr^{-1})**
	(A)	(B)
	Toolik Lake	
Baseline	3.79 ± 1.54	2.0
2.6	5.30 ± 2.16 (1.52/40%)	
4.5	6.24 ± 2.42 (2.45/65%)	
8.5	8.46 ± 4.23 (4.67/123%)	
	Lake E5	
Baseline	4.20 ± 1.52	1.4
2.6	5.87 ± 1.74 (1.67/40%)	
4.5	7.02 ± 2.12 (2.83/67%)	
8.5	9.61 ± 4.30 (5.41/129%)	
	Lake E1	
Baseline	8.43 ± 3.72	9.4
2.6	11.59 ± 4.82 (3.16/38%)	
4.5	13.66 ± 5.51 (5.23/62%)	
8.5	19.10 ± 9.46 (10.67/127%)	
	Lake E6	
Baseline	8.65 ± 4.01	13.3
2.6	11.91 ± 5.54 (3.26/38%)	
4.5	13.99 ± 6.01 (5.35/62%)	
8.5	19.70 ± 10.43 (11.05/128%)	

554

555 **Table 5.** Average air temperature from GCM data under baseline (1976-2005) and future scenarios
556 (2071-2100). Temperature changes from baseline are shown in parentheses.

GCM scenario	Mean air temperature (°C)
Baseline (1976-2005)	-7.96
2.6 *(2071-2100)*	-4.37 (3.59°C)
4.5 *(2071-2100)*	-2.86 (5.10°C)
8.5 *(2071-2100)*	0.67 (8.63°C)

557

558 The present study is distinct from Tan and Zhuang (2015) in that differing equations were
559 required to estimate the ebullitive flux from shallower ponds ($\mathbf{Z_{mean}}$ = ~1–3 m; E1, E6) and
560 deeper lakes ($\mathbf{Z_{mean}}$ = ~6–7 m; Table 1). They followed a similar approach to this study (water
561 and sediment thermodynamics, gas and bubble transport and a sediment gas module with CH_4
562 dynamics) to simulate five Arctic lakes (thermokarst lakes, yedoma/non-yedoma in
563 continuous/discontinuous permafrost), including Toolik Lake (the methods are described in Tan
564 et al. (2015)). Their maximum lake depths and surface areas, were similar to ours, ranging
565 between 2.9 to 25 m and 1 to 149 ha; however, no validation of CH_4 concentrations in Toolik
566 Lake and Goldstream Lake (64.9°N 147.7°W; maximum depth 2.9 m, area 1.0 ha) was
567 performed. Therefore, it was not possible to directly compare our model results with theirs.
568 Moreover, their $C_{labile,}$ was calibrated against data from a single shallow lake (Suchi Lake, 69ºN
569 161 ºE, maximum depth 11 m, area 5.8 ha), which is likely more productive than the deeper
570 systems (Bastviken et al., 2004; Wik, Varner and Walter Anthony, et al., 2016) and could result
571 in higher CH_4 fluxes. In the present study, C_{labile} was not altered between the baseline and future
572 simulations, under the assumption that temperature was the sole driver of increased flux (Eq. 4).
573 Changes in lake productivity may occur, particularly as permafrost melts, however, these effects
574 are beyond the scope of the present work.

575 The CH_4 flux estimates simulated in this study can be considered conservative (Table 4). We
576 note that GHG emissions from water bodies are not implemented in CMIP5, which means the
577 contribution of these natural systems to climate change is underestimated (Zhang et al., 2017),
578 causing both future warming and consequent CH_4 emissions to be greater than modelled herein
579 with CMIP5 forcing.

580 *Comparison to regional and global estimates.* Many studies extrapolate measured CH_4 fluxes
581 from a limited number of water bodies to enable regional or global-scale emission estimates
582 (Bastviken et al., 2004; DelSontro et al., 2018; Wik, Varner and Walter Anthony, et al., 2016).
583 This approach often employs short-term sampling that neglects the temporal dynamics of
584 processes that govern CH_4 production, oxidation, ebullition, gas exchange at the water-air
585 interface and oxic CH_4 production (Wik, Thornton and Bastviken, et al., 2016). Consequently,
586 there are significant discrepancies in total CH_4 emissions estimates within the literature. For
587 example, the process-based model by Tan and Zhuang (2015) estimated present-day fluxes from
588 lakes north of 60°N to be 23.66 Tg CH_4 yr^{-1} for a total lake area of 1.24 $\times 10^6$ km^2, while
589 observation-based (22 freshwater ecosystems) extrapolation results from Bastviken et al., (2011)
590 gave 13.4 Tg CH_4 yr^{-1} for lakes north of 54°N and a total area of 1.82 $\times 10^6$ km^2. In contrast,
591 Wik, Varner and Walter Anthony, et al., (2016) estimated 16.5 ± 9.2 Tg CH_4 yr^{-1} (total lake area

of 1.84×10^6 km^2), using data from 733 northern lakes and updated lake-area estimates, including annual emissions of 8.3 ± 4.7 Tg CH_4 yr^{-1} (total lake area of 1.45×10^6 km^2) from all glacial/post-glacial lakes.

Our study was limited to simple parameterizations of CH_4 fluxes from only four lakes; however, we were able to compute CH_4 emissions year-round on sub-daily timescales, as they responded to changes in simulated sediment temperature. Extrapolating the mean flux from the four simulated Alaskan lakes, using 1.45×10^6 km^2 of glacial/post-glacial lake area (Wik, Varner and Walter Anthony, et al., 2016), gives total baseline (1976–2005) CH_4 emissions of 9.1 Tg CH_4 yr^{-1}, which falls within 10% of the average updated estimate from Wik, Varner and Walter Anthony, et al., (2016). While these comparisons must be interpreted with caution, given our small sample size of 4 lakes, this result is interesting given that smaller lakes tend to have larger areal CH_4 emissions (Wik et al., 2002) and our largest lake, (Toolik) is in the fourth smallest lake-size class out of nine (Downing et al., 2006). Therefore, we likely overestimate the extrapolated flux, which lies in the lower range of the estimate from Wik, Varner and Walter Anthony, et al., (2016). This flux overestimation, based on lake size, may be compensated for by our underestimation relative to observed fluxes (Table 4).

Our simulations show that the effect of climate change on areal (per m^2) CH_4 fluxes was more pronounced in the shallower lakes (E1 and E6), in agreement with observations Wik, Varner and Walter Anthony, et al., (2016); however, overall emissions were much higher from the deeper lakes (Toolik and E5) due to their significantly larger surface area (e.g., Downing et al., 2006). For instance, the annual lake-wide surface flux (ebullition and diffusion) from Toolik Lake and Lake E5, respectively, were 5.64 and 0.46 Mg CH_4 yr^{-1} during 1976-2005. For RCP 8.5, emissions increased ~2 times for both lakes (to 12.60 and 1.04 Mg CH_4 yr^{-1}, respectively: Table 4). Fluxes from lakes E1 and E6, were 0.24 and 0.16 Mg CH_4 yr^{-1}, respectively, under baseline conditions, and also increased ~2 times under RCP 8.5 (to 0.55 and 0.37 Mg CH_4 yr^{-1}, respectively; Table 4). Notably, CH_4 emissions from these freshwater systems will remain above the 1976-2005 averages, even with a conservative estimate of climate-driven warming (RCP 2.6), which indicates the urgency to include the influence of these natural systems in GHG budgets and land surface schemes.

Comparison of simulated CH_4 emissions with observations. The differences between our simulations and observations (Table 4), can be partially attributed to the methods used to estimate seasonal and annual emissions. Sepulveda-Jauregui et al. (2015) note that there is uncertainty in their measurements since it is assumed that single-day diffusion measurements are representative of the entire ice-free season. However, they argue that this is the best (only) available data, and these are well-established practices, as described in Bastviken et al., (2011). This is to say that significant uncertainty amongst reported estimates of CH_4 emissions remains, which does not allow for an accurate comparison. The methods used to quantify CH_4 fluxes would ideally be near-continuous and evenly distributed in space. Certainly, attempts to improve spatial and temporal sampling techniques in the field and laboratory will assist future studies to obtain a more accurate representation of the overall CH_4 potential of lakes across the globe, especially regarding ebullitive fluxes, which are highly episodic.

Errors from neglecting downscaling. The GCM-forced model simulated lake temperature profiles – at times – showed notable differences from the observations (Table 3), particularly at

the lake bottom (Figure 2), relative to when the model was forced with observed meteorological data. To assess the impacts of the discrepancy in simulated bottom lake temperature, it is important to compare the differences ebullitive and diffusive fluxes calculated under the different model forcing conditions. For 2004 (Jul. 5 to Aug. 19) in Lake E5, a difference of 5.31 °C was modelled between the average bottom temperature calculated with the observed meteorological data and the long-term GCM-forced simulation (6.77°C and 12.09°C, respectively; Figure 2). For this period, the average ebullitive fluxes (Eq. 1) were 2.36 mg CH_4 m^{-2} d^{-1} (observed meteorological forcing) and 13.00 mg CH_4 m^{-2} d^{-1} (long-term GCM forcing). The seasonal average diffusive fluxes (Eq. 4) were 3.55 mg CH_4 m^{-2} d^{-1} (observed meteorological forcing) and 39.84 mg CH_4 m^{-2} d^{-1} (long-term GCM forcing). This warm bias (Figure 2) led to an overestimation of the surface CH_4 flux (1.40 g CH_4 m^{-2} yr^{-1} observed in 2011–2012 vs. 4.20 g CH_4 m^{-2} yr^{-1} simulated over 1976-2005). To minimize these effects on the interpretation of the results, we computed percentage changes between the GCM-forced baseline and GCM-forced future projections (Table 6), considering that both simulations are subject to the bias and aggregation error. This approach is well established for assessing the simulated impacts of climate change (e.g., Plummer et al. 2006).

Model scalability and transferability. The temperature and CH_4 models were designed to have scalable parameterizations (which can be applied to many lakes based on a minimal number of readily available lake parameters, e.g., Table 1). However, transferability of the models to other lakes on the land surface, without the need for recalibration must be tested. Mackay (2012) found differences in lake surface temperatures to largely result from differences in surface area, depth, and transparency (all scalable model parameters; Table 1). Moreover, transferability of CSLM was shown where simulations of Canadian boreal, Alaskan Arctic and Swedish boreal lakes had some error but did not require parameter tuning or other model adjustments, which is essential for regional or global application. The present study was not designed to test model transferability. We found that bottom temperatures were dependent on the surface wind drag (as controlled by adjusting the wind sensor height). This may be a direct result of using a single set of observed meteorological data for all the lakes, which cover a ~5 km geographical region (Figure 1) and CRCM forcing data from a 50 km grid (e.g., variability in wind sheltering) or poor specification of sediment heating (MacKay 2019). Therefore, application of the model to more lakes should be undertaken to better understand the need for individual lake calibration to improve transferability in simulating sediment temperatures.

The CH_4 model was more transferable than the temperature model. For the diffusive flux, the same C_{labile}, K_z and k_{ox} were used with all four lakes (Table 2). However, for the two larger and deeper lakes (Toolik and E5, Z_{mean} ~ 6–7 m and 10–150 ha), the ebullitive fluxes were estimated from Arctic lake data using Eq. 1, which is a scalable parameterization based on the simulated sediment temperature (Table 1). However, this parameterization was inappropriate for the smaller shallower lakes (E1 and E6, Z_{mean} ~ 1–3 m and 2–3 ha), which required an ebullition equation developed for shallow boreal ponds. Observations show shallower systems (ponds < ~3 m depth) to have CH_4 fluxes ~10 times greater than deeper systems (lakes ~3–30 m depth), supporting our usage of a different parameterization for ponds (Wik, Varner and Walter Anthony, et al. 2016). Further research is required to test if Eq. 1 is transferable to lakes larger than Toolik and E5. Ebullition flux equations should also be developed for shallower Arctic lakes like E1 and E6 (Aben et al., 2017).

679 # 5 Conclusions

680 This study evaluated the ability of a computational one-dimensional CH_4 model to estimate
681 historical, near present-day and future emissions from four Alaskan lakes, when forced with raw
682 (not downscaled) output data from a GCM. The GCM overestimated the bottom lake
683 temperature, which was subsequently used in the CH_4 sub-model. Simulated temperature error
684 metrics against observations were better when using observed meteorological forcing, compared
685 to raw GCM forcing (RMSE = 0.38 to 0.90 °C vs. 1.03 to 3.50 °C; R^2 = 0.97 to 0.99 vs. 0.74 to
686 0.81). There was no discernable difference in metrics for 2004 GCM vs. 1976–2005 GCM
687 forcing, indicating long term model drift was not an obvious source of error. Similar to previous
688 studies (Mackay, 2012), we found that CLASS simulated temperatures to be transferable (~1 °C
689 RMSE) between lakes without re-calibration; however, site specific adjustment of the wind
690 stress was required. This was also the case for the CH_4 fluxes from the deeper lakes (~6–7 m
691 mean depth); however, the shallower (~1–3 m mean depth) required an ebullition equation
692 derived from Boreal ponds. Future work should focus on improving simulation of bottom water
693 (sediment) temperatures, accounting for hypsometry that includes sediment area in littoral zones
694 where ebullition is maximal and developing transferable CH_4 flux parameterizations for shallow
695 Arctic lakes (~1–3 m mean depth).

696 The three climate warming scenarios (RCPs 2.6, 4.5 and 8.5) all resulted in a significant increase
697 in total CH_4 emissions averaged over 2071–2100, relative to 1976–2005 (38–129%). However,
698 RCP 2.6 and 4.5 will lead to stabilized Arctic lake temperatures and CH_4 emissions by 2100, at
699 levels 0.61 – 1.21°C and 38–67%, respectively, above the 1976–2005 averages. Overall
700 emissions from the larger two lakes (6–7 m mean depth and 10–150 ha) were modelled to be
701 higher in comparison to those from the smaller two systems (1–3 m mean depth and 2–3 ha) due
702 to their larger surface area; however, areal fluxes were larger from the smaller shallower lakes.
703 Results from this work corroborate the urgent need to include the contributions of GHGs from
704 freshwater systems in regional and global climate models and associated positive feedback with
705 increased sediment temperatures.

706 **Table 6.** Summary of simulated mean ± standard deviation of model output forced with GCM data under baseline (1976-2005) and future
707 scenarios (2071-2100). Temperature and absolute/percentage change from baseline for CH_4 fluxes and ice-free days are shown in parentheses.
708

	Bottom lake temperature (°C)	**Sediment diffusive flux (mg CH_4 m^{-2} d^{-1})**	**Sediment ebullitive flux (mg CH_4 m^{-2} d^{-1})**	**Total surface flux (mg CH_4 m^{-2} d^{-1})**	**Ice-free days**
	(A)	(B)	(C)	(D)	(E)
	Toolik Lake ($k_{Ox} = 1.74\times10^{-5}$ s^{-1})				
Baseline	3.61 ± 0.70	42.03 ± 3.88	1.65 ± 0.41	10.38 ± 1.54	110.86 ± 8.63
2.6	4.24 ± 0.78 (0.63)	47.86 ± 4.76 (5.83/14%)	2.68 ± 0.60 (1.04/63%)	14.53 ± 2.16 (4.15/40%)	128.83 ± 6.70 (17.97/16%)
4.5	4.55 ± 0.68 (0.94)	51.55 ± 3.92 (9.52/23%)	3.39 ± 0.66 (1.74/106%)	17.10 ± 2.42 (6.73/65%)	134.97 ± 9.39 (24.10/22%)
8.5	5.43 ± 0.66 (1.82)	62.10 ± 6.36 (20.07/48%)	5.21 ± 0.96 (3.57/217%)	23.17 ± 4.23 (12.79/123%)	154.66 ± 10.98 (43.79/40%)
	Lake E5 ($k_{Ox} = 1.74\times10^{-5}$ s^{-1})				
Baseline	3.16 ± 0.47	40.24 ± 3.02	1.76 ± 0.50	11.50 ± 1.52	111.76 ± 8.65
2.6	3.77 ± 0.44 (0.61)	45.87 ± 3.37 (5.62/14%)	2.77 ± 0.55 (1.01/57%)	16.08 ± 1.74 (4.57/40%)	129.83 ± 6.57 (18.07/16%)
4.5	4.28 ± 0.51 (1.12)	50.68 ± 3.74 (10.44/26%)	3.51 ± 0.64 (1.75/99%)	19.24 ± 2.12 (7.74/67%)	135.34 ± 8.90 (23.59/21%)
8.5	5.12 ± 0.57 (1.95)	61.28 ± 6.25 (21.03/52%)	5.43 ± 1.04 (3.67/208%)	26.32 ± 4.30 (14.81/129%)	154.93 ± 11.26 (43.17/39%)
	Lake E1 ($k_{Ox} = 1.74\times10^{-5}$ s^{-1})				
Baseline	3.41 ± 0.42	43.94 ± 4.12	10.92 ± 1.75	23.09 ± 3.72	105.55 ± 9.42
2.6	4.25 ± 0.42 (0.84)	52.19 ± 5.73 (8.25/19%)	14.41 ± 2.83 (3.48/32%)	31.76 ± 4.82 (8.66/38%)	123.24 ± 6.15 (17.69/17%)
4.5	4.61 ± 0.51 (1.20)	57.20 ± 6.09 (13.27/30%)	16.74 ± 3.01 (5.82/53%)	37.42 ± 5.51 (14.33/62%)	129.21 ± 9.42 (23.66/22%)
8.5	5.55 ± 0.63 (2.14)	71.00 ± 9.42 (27.07/62%)	23.52 ± 5.12 (12.59/115%)	52.33 ± 9.46 (29.24/127%)	148.86 ± 11.57 (43.31/41%)
	Lake E6 ($k_{Ox} = 1.74\times10^{-5}$ s^{-1})				
Baseline	3.30 ± 0.37	44.09 ± 4.23	11.11 ± 1.86	23.69 ± 4.01	103.24 ± 9.57
2.6	4.12 ± 0.39 (0.82)	52.46 ± 6.10 (8.36/19%)	14.71 ± 3.08 (3.59/32%)	32.63 ± 5.54 (8.94/38%)	122.28 ± 5.85 (19.03/18%)
4.5	4.51 ± 0.43 (1.21)	57.60 ± 6.31 (13.51/31%)	17.10 ± 3.23 (5.99/54%)	38.34 ± 6.01 (14.64/62%)	127.83 ± 9.31 (24.59/24%)
8.5	5.55 ± 0.58 (2.24)	72.03 ± 10.05 (27.94/63%)	24.23 ± 5.75 (13.12/118%)	53.98 ± 10.43 (30.29/128%)	147.41 ± 11.85 (44.17/43%)

709

Acknowledgements

We thank Murray MacKay for helping with the CSLM code and providing the future climate model output. Sally MacIntyre and Alicia Cortes are thanked for providing field data. Kevin Mumford and Melissa Lafrenière provided comments on a draft version of the manuscript. The research was funded by NSERC Discovery and Discovery Accellerator Supplement grants to LB. HH was funded by the Ontario/Baden-Württemberg Faculty Mobility Program and the German Research Foundation DFG grant: HO 4536/4-1.

Data Availability Statement

Weather data, temperature time-series, CH_4 time-series were obtained from ARC LTER, NSF Arctic Data Center site (https://arcticdata.io/catalog/view/doi:10.18739/A2X54S) and the Environmental Data Center site of the Toolik Field Station in Alaska (https://arc-lter.ecosystems.mbl.edu/; refer to reference list for specific yearly data). The second version of the CSLM source code is available at https://github.com/MurrayMackay/CSLM. All remaining relevant data supporting the conclusions of this study are included in the article and supplementary material. Further inquiries can be directed to the corresponding author.

References

Aben, R. C. H., Barros, N., van Donk, E., Frenken, T., Hilt, S., Kazanjian, G., Kosten, S. (2017) et al. Cross continental increase in methane ebullition under climate change. Nature Communications, 8(1), 1–8. https://doi.org/10.1038/s41467-017-01535-y

Bastviken, D., Tranvik, L. J., Downing, J. A., Crill, P. M., & Enrich-Prast, A. (2011). Freshwater Methane Emissions Offset the Continental Carbon Sink. Science, 331(6013), 50–50. https://doi.org/10.1126/science.1196808

Bastviken, David, Cole, J., Pace, M., & Tranvik, L. (2004). Methane emissions from lakes: Dependence of lake characteristics, two regional assessments, and a global estimate. Global Biogeochemical Cycles, 18(4), GB4009. https://doi.org/10.1029/2004GB002238

Bastviken, David, Ejlertsson, J., & Tranvik, L. (2002). Measurement of Methane Oxidation in Lakes: A Comparison of Methods. Environmental Science & Technology, 36(15), 3354–3361. https://doi.org/10.1021/es010311p

Belkin, I. M. (2009). Rapid warming of Large Marine Ecosystems. Progress in Oceanography, 81(1–4), 207–213. https://doi.org/10.1016/j.pocean.2009.04.011

Bintanja, R. (2018). The impact of Arctic warming on increased rainfall. Scientific Reports, 8(1), 16001. https://doi.org/10.1038/s41598-018-34450-3

Boegman, L., Loewen, M., Hamblin, P., & Culver, D. (2001). Application of a two-dimensional hydrodynamic reservoir model to Lake Erie. Canadian Journal of Fisheries and Aquatic Sciences, 58(5), 858-869. doi: 10.1139/f01-035

Boegman, L., & Sleep, S. (2012). Feasibility of Bubble Plume Destratification of Central Lake Erie. *Journal of Hydraulic Engineering*, 138(11), 985–989. https://doi.org/10.1061/(ASCE)HY.1943-7900.0000626

Bolkhari, H., Boegman, L., & Smith, R. (2021). Simulated impacts of climate change on Lake Simcoe water quality. Inland Waters, 12(2), 215-231. doi: 10.1080/20442041.2021.1969190

Denfeld, B. A., Baulch, H. M., del Giorgio, P. A., Hampton, S. E., & Karlsson, J. (2018). A synthesis of carbon dioxide and methane dynamics during the ice-covered period of Northern Lakes. *Limnology and Oceanography Letters*, 3(3), 117–131. https://doi.org/10.1002/lol2.10079

Dagurova, O. P., Namsaraev, B. B., Kozyreva, L. P., Zemskaya, T. I., & Dulov, L. E. (2004). Bacterial Processes of the Methane Cycle in Bottom Sediments of Lake Baikal. Microbiology, 73(2), 202–210. https://doi.org/10.1023/B:MICI.0000023990.71983.c1

Dean, W. E., & Gorham, E. (1998). Magnitude and significance of carbon burial in lakes, reservoirs, and peatlands. Geology, 26(6), 535. https://doi.org/10.1130/0091-7613(1998)026<0535:MASOCB>2.3.CO;2

DelSontro T., del Giorgio P., Prairie Y. Going Beyond the Mean: Using Empirical Models to Upscale and Predict Aquatic Boreal CH4 Emissions in a Warming World. Poster presented at the AGU Fall Meeting. San Francisco; 2009 December 9–13; San Francisco, CA. USA. https://agu.confex.com/agu/fm19/meetingapp.cgi/Paper/587117

767 DelSontro, T., Beaulieu, J. J., & Downing, J. A. (2018). Greenhouse gas emissions from lakes
768 and impoundments: Upscaling in the face of global change. Limnology and Oceanography
769 Letters, 3(3), 64–75. https://doi.org/10.1002/lol2.10073

770 DelSontro, T., Boutet, L., St-Pierre, A., del Giorgio, P. A., & Prairie, Y. T. (2016). Methane
771 ebullition and diffusion from northern ponds and lakes regulated by the interaction between
772 temperature and system productivity. Limnology and Oceanography, 61(S1), S62–S77.
773 https://doi.org/10.1002/lno.10335

774 Downing, J. A., Prairie, Y. T., Cole, J. J., Duarte, C. M., Tranvik, L. J., Striegl, R. G., …
775 Middelburg, J. J. (2006). The global abundance and size distribution of lakes, ponds, and
776 impoundments. Limnology and Oceanography, 51(5), 2388–2397.

777 Eugster, W. *et al.* (2020) "Interannual, summer, and diel variability of CH4and co2effluxes from
778 Toolik Lake, Alaska, during the ice-free periods 2010–2015," *Environmental Science: Processes
779 & Impacts* [Preprint]. https://doi.org/10.1039/d0em00125b.

780 Giblin, A. E., & Kling, G. (2015). Physical and chemical data for various lakes near Toolik
781 Research Station, Arctic LTER. Summer 1983 to 1989. Environmental Data Initiative.
782 https://doi.org/http://dx.doi.org/10.6073/pasta/1f780cc1b9e31f58a87d72b8eb2693ea

783 Graversen, R. G., Mauritsen, T., Tjernström, M., Källén, E., & Svensson, G. (2008). Vertical
784 structure of recent Arctic warming. Nature, 451(7174), 53–56.
785 https://doi.org/10.1038/nature06502

786 Greene, S., Walter Anthony, K. M., Archer, D., Sepulveda-Jauregui, A., & Martinez-Cruz, K.
787 (2014). Modeling the impediment of methane ebullition bubbles by seasonal lake ice.
788 Biogeosciences, 11(23), 6791–6811. https://doi.org/10.5194/bg-11-6791-2014

789 Golub, M., Thiery, W., Marcé, R., Pierson, D., Vanderkelen, I., & Mercado-Bettin, D. et al.
790 (2022). A framework for ensemble modelling of climate change impacts on lakes worldwide: the
791 ISIMIP Lake Sector. Geoscientific Model Development, 15(11), 4597-4623. doi: 10.5194/gmd-
792 15-4597-2022

793 Happell, J. D., Chanton, J. P., & Showers, W. J. (1995). Methane transfer across the water-air
794 interface in stagnant wooded swamps of Florida: Evaluation of mass-transfer coefficients and
795 isotropic fractionation. Limnology and Oceanography, 40(2), 290–298.
796 https://doi.org/10.4319/lo.1995.40.2.0290

797 Harriss, R., Bartlett, K., Frolking, S., & Crill, P. (1993). Methane Emissions from Northern
798 High-Latitude Wetlands. In Biogeochemistry of Global Change (pp. 449–486).
799 https://doi.org/10.1007/978-1-4615-2812-8_25

800 Hobbie, J. E., & Kling, G. W. (2014). Alaska's Changing Arctic – Ecological Consequences for
801 Tundra, Streams, and Lakes (John E. Hobbie & G. W. Kling, Eds.).
802 https://doi.org/10.1093/acprof:osobl/9780199860401.001.0001

803 Holmes, J. (2001). Wind Loading of Structures. https://doi.org/10.4324/9780203301647

804 Huang, A., Rao, Y. R., & Lu, Y. (2010). Evaluation of a 3-D hydrodynamic model and
805 atmospheric forecast forcing using observations in Lake Ontario. Journal of Geophysical
806 Research, 115(C2), C02004. https://doi.org/10.1029/2009JC005601

Hurtado Caicedo, D., Modelling Methane Emissions from Arctic Lakes. (Master's thesis, Queen's University). Available from QSPACE portal. (URI: http://hdl.handle.net/1974/27470)

Jabbari, A., Boegman, L., Mackay, M., Hadley, K., Paterson, A., Jeziorski, A., … Smol, J. (2016). Long-term simulations of dissolved oxygen concentrations in Lake Trout lakes. (April), 2–3. https://doi.org/10.13140/RG.2.1.1915.6889

Jorgenson, M. T., Romanovsky, V., Harden, J., Shur, Y., O'Donnell, J., Schuur, E. A. G., … Marchenko, S. (2010). Resilience and vulnerability of permafrost to climate change. Canadian Journal of Forest Research, 40(7), 1219–1236. https://doi.org/10.1139/X10-060

Juutinen, S., Rantakari, M., Kortelainen, P., Huttunen, J. T., Larmola, T., Alm, J., … Martikainen, P. J. (2009). Methane dynamics in different boreal lake types. Biogeosciences, 6(2), 209–223. https://doi.org/10.5194/bg-6-209-2009

Karlsson, J., Giesler, R., Persson, J., & Lundin, E. (2013). High emission of carbon dioxide and methane during ice thaw in high latitude lakes. Geophysical Research Letters, 40(6), 1123–1127. https://doi.org/10.1002/grl.50152

Kessler, M. A., Plug, L. J., & Walter Anthony, K. M. (2012). Simulating the decadal- to millennial-scale dynamics of morphology and sequestered carbon mobilization of two thermokarst lakes in NW Alaska. Journal of Geophysical Research: Biogeosciences, 117(1), 1–22. https://doi.org/10.1029/2011JG001796

Kling, G.W., Kipphut, G.W. and Miller, M.C. (1992) "The flux of CO2 and ch4 from lakes and rivers in Arctic Alaska," *Hydrobiologia*, 240(1-3), pp. 23–36. https://doi.org/10.1007/bf00013449.

Kling, G. (2000). Meteorological data collected on Toolik Lake during the ice free season since 1989 to 2009, Arctic LTER, Toolik Research Station, Alaska. Environmental Data Initiative. https://doi.org/http://dx.doi.org/10.6073/pasta/35a48d475054bb60dcc0de3bd199be40

Lin, S., Boegman, L., Jabbari, A., Valipour, R., and Zhao, Y. (2022). Observation and parameterization of bottom shear stress and sediment resuspension in a large shallow lake. Limnology and Oceanography (Submitted).

Lofton, D., Whalen, S., & Hershey, A. (2013). Effect of temperature on methane dynamics and evaluation of methane oxidation kinetics in shallow Arctic Alaskan lakes. Hydrobiologia, 721(1), 209-222. doi: 10.1007/s10750-013-1663-x

MacIntyre, S. (2003). Time-series of 5 minute water temperatures averages from Toolik Lake, Toolik Field Station, Alaska, Summer 2001. Environmental Data Initiative. https://doi.org/http://dx.doi.org/10.6073/pasta/f842ce68841a01c3cb92ea068417d4af

(2004). Time-series of 5 minute water temperatures averages from Toolik Lake, Toolik Field Station, Alaska, Summer 2002. Environmental Data Initiative. https://doi.org/http://dx.doi.org/10.6073/pasta/dbae1b80e0e2460dd9f3354477ec211c

(2005). Time-series of 5 minute water temperatures averages from Toolik Lake, Toolik Field Station, Alaska, Summer 2003. Environmental Data Initiative. https://doi.org/http://dx.doi.org/10.6073/pasta/4a136995016fab673b5992ceea6f3a57

(2006). Water temperatures from Toolik Lake in Summer 2004. Environmental Data Initiative. https://doi.org/http://dx.doi.org/10.6073/pasta/3fdd4c2d590d5485770e031d7e8678d8

(2007). Time-series of 5 minute water temperatures averages from Toolik Lake, Toolik Field Station, Alaska, Summer 2005. Environmental Data Initiative. https://doi.org/http://dx.doi.org/10.6073/pasta/0892203589595da10989458b6c59b6f1

(2009). Time-series of 5 minute water temperatures averages from Toolik Lake, Toolik Field Station, Alaska, Summer 2007. Environmental Data Initiative. https://doi.org/http://dx.doi.org/10.6073/pasta/12eb98a258a58ad48867796798bd815d

(2012). Time-series of 5 minute water temperatures averages from Lake E5 near Toolik Field Station, Alaska Summer 2001. Environmental Data Initiative. https://doi.org/http://dx.doi.org/10.6073/pasta/58ac3c3cc56f45190a60ba5a399e8c9d

(2015a). Time-series of 5 minute water temperatures averages from Lake E5 near Toolik Field Station, Alaska Summer 2002. Environmental Data Initiative. https://doi.org/http://dx.doi.org/10.6073/pasta/c9ba44741c6859fd9a1abc509c06ba1a

(2015b). Time-series of 5 minute water temperatures averages from Lake E5 near Toolik Field Station, Alaska Summer 2003. Environmental Data Initiative. https://doi.org/http://dx.doi.org/10.6073/pasta/c3b858f1bc3bfd6c375524f6168be35f

(2015c). Time-series of 5 minute water temperatures averages from Lake E5 near Toolik Field Station, Alaska Summer 2004. Environmental Data Initiative. https://doi.org/http://dx.doi.org/10.6073/pasta/e057c34d84aaed1db7a0089ed7d3fd21

(2015d). Time-series of 5 minute water temperatures averages from Lake E5 near Toolik Field Station, Alaska Summer 2005. Environmental Data Initiative. https://doi.org/http://dx.doi.org/10.6073/pasta/94cc2e0f6a7f26654e3cae655d5c7cc1

(2015e). Time-series of 5 minute water temperatures averages from Lake E6 near Toolik Field Station, Alaska Summer 2003. Environmental Data Initiative. https://doi.org/http://dx.doi.org/10.6073/pasta/5ba23933c1b499e423dd9f4967c26684

(2015f). Time-series of 5 minute water temperatures averages from Lake E6 near Toolik Field Station, Alaska Summer 2004. Environmental Data Initiative. https://doi.org/http://dx.doi.org/10.6073/pasta/558a26a196417102957047ae1b7c31fd

(2015g). Time-series of 5 minute water temperatures averages from Lake E6 near Toolik Field Station, Alaska Summer 2007. Environmental Data Initiative. https://doi.org/http://dx.doi.org/10.6073/pasta/f0fd60dcf9ce17971de630a92b6c80d2

(2015h). Time-series of 5 minute water temperatures averages from Lake E6 near Toolik Field Station, Alaska Summerr 2005. Environmental Data Initiative. https://doi.org/http://dx.doi.org/10.6073/pasta/051e6f0681b1a05d06f1516d448d83b8

MacIntyre, S., & Cortés, A. (2017). Time series of water temperature, specific conductance, and oxygen from Toolik Lake, and Lakes E1, E5, E6, and N2, North Slope, Alaska. Arctic Data Center. https://doi.org/10.18739/A2X54S

MacIntyre, S., Cortés, A., & Sadro, S. (2018). Sediment respiration drives circulation and production of CO 2 in ice-covered Alaskan arctic lakes. Limnology and Oceanography Letters, 3(3), 302–310. https://doi.org/10.1002/lol2.10083

MacIntyre, S., Sickman, J. O., Goldthwait, S. A., & Kling, G. W. (2006). Physical pathways of nutrient supply in a small, ultraoligotrophic arctic lake during summer stratification. Limnology and Oceanography, 51(2), 1107–1124. https://doi.org/10.4319/lo.2006.51.2.1107

MacKay, M. D., Neale, P. J., Arp, C. D., de Senerpont Domis, L. N., Fang, X., Gal, G., … Stokes, S. L. (2009). Modeling lakes and reservoirs in the climate system. Limnology and Oceanography, 54(6 PART 2), 2315–2329. https://doi.org/10.4319/lo.2009.54.6_part_2.2315

MacKay, M. D. (2012). A Process-Oriented Small Lake Scheme for Coupled Climate Modeling Applications. Journal of Hydrometeorology, 13(6), 1911–1924. https://doi.org/10.1175/JHM-D-11-0116.1

MacKay, M. D., Verseghy, D. L., Fortin, V., & Rennie, M. D. (2017). Wintertime Simulations of a Boreal Lake with the Canadian Small Lake Model. *Journal of Hydrometeorology*, 18(8), 2143–2160. https://doi.org/10.1175/JHM-D-16-0268.1

MacKay, M.D. (2019). Incorporating wind sheltering and sediment heat flux into 1-D models of small boreal lakes: A case study with the Canadian Small Lake Model v2.0. Manuscript under review for journal *Geosci. Model Dev*. Available at: https://doi.org/10.5194/gmd-2018-258

Martinez-Cruz, K., Sepulveda-Jauregui, A., Walter Anthony, K., & Thalasso, F. (2015). Geographic and seasonal variation of dissolved methane and aerobic methane oxidation in Alaskan lakes. *Biogeosciences,* 12(15), 4595-4606. doi: 10.5194/bg-12-4595-2015

McGinnis, D. F., Greinert, J., Artemov, Y., Beaubien, S. E., & Wüest, A. (2006). Fate of rising methane bubbles in stratified waters: How much methane reaches the atmosphere? *Journal of Geophysical Research: Oceans,* 111(9), 1–15. https://doi.org/10.1029/2005JC003183

Meinshausen, M., Smith, S.J., Calvin, K., Daniel, J.S., Kainuma, M.L.T., Lamarque, J.-F., Matsumoto, K., Montzka, S.A., Raper, S.C.B., Riahi, K., Thomson, A., Velders, G.J.M., van Vuuren, D.P.P., 2011. The RCP greenhouse gas concentrations and their extensions from 1765 to 2300. Climatic Change 109, 213–241. https://doi.org/10.1007/s10584-011-0156-z

Michmerhuizen, C. M., Striegl, R. G., & McDonald, M. E. (1996). Potential methane emission from north-temperate lakes following ice melt. Limnology and Oceanography, 41(5), 985–991. https://doi.org/10.4319/lo.1996.41.5.0985

Nakhaei, N., Boegman, L., & Bouffard, D. (2016). Measurement of vertical oxygen flux in lakes from microstructure casts. 8th Int. Symp. on Stratified Flows, San Diego, USA, August 29 – September 1.

Nakhaei, N., Boegman, L., Mehdizadeh, M., & Loewen, M. (2018). Hydrodynamic modeling of Edmonton storm-water ponds. Environmental Fluid Mechanics, 19(2), 305–327. https://doi.org/10.1007/s10652-018-9625-5

O'Brien, W. J. (1992). Toolik Lake: Ecology of an Aquatic Ecosystem in Arctic Alaska (W. J. O'Brien, Ed.). https://doi.org/10.1007/978-94-011-2720-2

O'Connor, D. J. (1983). Wind Effects on Gas-Liquid Transfer Coefficients. Journal of Environmental Engineering, 109(3), 731–752. https://doi.org/10.1061/(ASCE)0733-9372(1983)109:3(731)

Paturi, S., Boegman, L., & Rao, Y. R. (2012). Hydrodynamics of eastern Lake Ontario and the upper St. Lawrence River. *Journal of Great Lakes Research*, 38, 194–204.https://doi.org/10.1016/j.jglr.2011.09.008

Peeters, F., Encinas Fernandez, J., & Hofmann, H. (2019). Sediment fluxes rather than oxic methanogenesis explain diffusive CH4 emissions from lakes and reservoirs. *Scientific Reports*, 9(1), 243. https://doi.org/10.1038/s41598-018-36530-w

Phelps, A. R., Peterson, K. M., & Jeffries, M. O. (1998a). Methane efflux from high-latitude lakes during spring ice melt. Journal of Geophysical Research: Atmospheres, 103(D22), 29029–29036. https://doi.org/10.1029/98JD00044

Phelps, A. R., Peterson, K. M., & Jeffries, M. O. (1998b). Methane efflux from high-latitude lakes during spring ice melt. Journal of Geophysical Research: Atmospheres, 103(D22), 29029–29036. https://doi.org/10.1029/98JD00044

Plummer, D.A., Caya, D., Frigon, A., Côté, H., Giguère, M., Paquin, D., Biner, S., Harvey, R. and De Elia, R. (2006). Climate and climate change over North America as simulated by the Canadian RCM. Journal of Climate, 19(13), 3112-3132.

Randall, D.A., R.A. Wood, S. Bony, R. Colman, T. Fichefet, J. Fyfe, V. Kattsov, A. Pitman, J. Shukla, J. Srinivasan, R.J. Stouffer, A. Sumi and K.E. Taylor, 2007: Cilmate Models and Their Evaluation. In: Climate Change 2007: The Physical Science Basis. Contribution of Working Group I to the Fourth Assessment Report of the Intergovernmental Panel on Climate Change. Cambridge University Press, Cambridge, United Kingdom and New York, NY, USA.

Scalo, C., Boegman, L., & Piomelli, U. (2013). Large-eddy simulation and low-order modeling of sediment-oxygen uptake in a transitional oscillatory flow. Journal of Geophysical Research: Oceans, 118(4), 1926–1939. https://doi.org/10.1002/jgrc.20113

Schmid, M., de Batist, M., Granin, N. G., Kapitanov, V. A., McGinnis, D. F., Mizandrontsev, I. B., … Wüest, A. (2007). Sources and sinks of methane in Lake Baikal: A synthesis of measurements and modeling. Limnology and Oceanography, 52(5), 1824–1837. https://doi.org/10.4319/lo.2007.52.5.1824

Schwefel, R., Steinsberger, T., Bouffard, D., Bryant, L. D., Müller, B., & Wüest, A. (2018). Using small-scale measurements to estimate hypolimnetic oxygen depletion in a deep lake. Limnology and Oceanography, 63(S1), S54–S67. https://doi.org/10.1002/lno.10723

Sepulveda-Jauregui, A., Walter Anthony, K. M., Martinez-Cruz, K., Greene, S., & Thalasso, F. (2015). Methane and carbon dioxide emissions from 40 lakes along a north-south latitudinal transect in Alaska. Biogeosciences, 12(11), 3197–3223. https://doi.org/10.5194/bg-12-3197-2015

Stepanenko, V. M., Machul'skaya, E. E., Glagolev, M. v., & Lykossov, V. N. (2011). Numerical modeling of methane emissions from lakes in the permafrost zone. *Izvestiya, Atmospheric and Oceanic Physics*, *47*(2), 252–264. https://doi.org/10.1134/S0001433811020113

Stepanenko, V., Mammarella, I., Ojala, A., Miettinen, H., Lykosov, V., & Vesala, T. (2016). LAKE 2.0: A model for temperature, methane, carbon dioxide and oxygen dynamics in lakes. *Geoscientific Model Development*, 9(5), 1977–2006. https://doi.org/10.5194/gmd-9-1977-2016

Stocker, T.F., D. Qin, G.-K. Plattner, M. Tignor, S.K. Allen, J. Boschung, A. Nauels, Y. Xia, V. Bex and P.M. Midgley (eds.; IPCC, 2013): Climate Change 2013: The Physical Science Basis.

967 Contribution of Working Group I to the Fifth Assessment Report of the Intergovernmental Panel
968 on Climate Change. Cambridge University Press, Cambridge, United Kingdom and New York,
969 NY, USA, 1535 pp.

970 Stuckey, J., Noguera, J., Reyce, B., & Rowan, M. (2019). Bathymetric data from Alaskan Lakes,
971 Toolik Field Station, Alaska (2006-2015). *Arctic Data Center*.

972 Tan, Z., & Zhuang, Q. (2015). Arctic lakes are continuous methane sources to the atmosphere
973 under warming conditions. *Environmental Research Letters*, *10*(5), 054016.
974 https://doi.org/10.1088/1748-9326/10/5/054016

975 Tan, Z., Zhuang, Q., & Walter Anthony, K. (2015). Modeling methane emissions from arctic
976 lakes: Model development and site-level study. *Journal of Advances in Modeling Earth Systems*,
977 *7*(2), 459–483. https://doi.org/10.1002/2014MS000344

978 Thottathil, S., Reis, P., & Prairie, Y. (2019). Methane oxidation kinetics in northern freshwater
979 lakes. *Biogeochemistry*, 143(1), 105-116. doi: 10.1007/s10533-019-00552-x

980 Verseghy, D. L., & MacKay, M. D. (2017). Offline Implementation and Evaluation of the
981 Canadian Small Lake Model with the Canadian Land Surface Scheme over Western Canada.
982 *Journal of Hydrometeorology*, 18(6), 1563–1582. https://doi.org/10.1175/JHM-D-16-0272.1

983 Walter Anthony, K. M., & Anthony, P. (2013). Constraining spatial variability of methane
984 ebullition seeps in thermokarst lakes using point process models. *Journal of Geophysical*
985 *Research: Biogeosciences*, *118*(3), 1015–1034. https://doi.org/10.1002/jgrg.20087

986 Walter, K., Smith, L., & Stuart Chapin, F. (2007). Methane bubbling from northern lakes:
987 present and future contributions to the global methane budget. *Philosophical Transactions Of*
988 *The Royal Society A: Mathematical, Physical And Engineering Sciences*, 365(1856), 1657-1676.
989 doi: 10.1098/rsta.2007.2036

990 Walter Anthony, K. M., Vas, D. A., Brosius, L., Chapin, F. S., I., Zimov, S. A., & Zhuang, Q.
991 (2010). Estimating methane emissions from northern lakes using ice bubble surveys. *Limnology*
992 *and Oceanography: Methods,* 8(NOV), 592–609. https://doi.org/10.4319/lom.2010.8.0592

993 Walter Anthony, K. M., Engram, M., Duguay, C. R., Jeffries, M. O., & Chapin, F. S. (2008). The
994 Potential Use of Synthetic Aperture Radar for Estimating Methane Ebullition From Arctic Lakes
995 1. *JAWRA Journal of the American Water Resources Association*, *44*(2), 305–315.
996 https://doi.org/10.1111/j.1752-1688.2007.00163.x

997 Walter Anthony, K. M., Zimov, S. A., Chanton, J. P., Verbyla, D., & Chapin, F. S. (2006).
998 Methane bubbling from Siberian thaw lakes as a positive feedback to climate warming. *Nature*,
999 *443*(7107), 71–75. https://doi.org/10.1038/nature05040

1000 Whalen, S. C. (2005). Biogeochemistry of Methane Exchange between Natural Wetlands and the
1001 Atmosphere. *Environmental Engineering Science*, *22*(1), 73–94.
1002 https://doi.org/10.1089/ees.2005.22.73

1003 Wiesenburg, D. A., & Guinasso, N. L. (1979). Equilibrium Solubilities of Methane, Carbon
1004 Monoxide, and Hydrogen in Water and Sea Water. *Journal of Chemical and Engineering Data*,
1005 *24*(4), 356–360. https://doi.org/10.1021/je60083a006

1006 Wik, M. (2016). *Emission of methane from northern lakes and ponds* (Doctoral thesis,
1007 Stockholm University). Available from DiVA portal. (URN: urn:nbn:se:su:diva-126823)

Wik, M., Crill, P. M., Varner, R. K., & Bastviken, D. (2013). Multiyear measurements of ebullitive methane flux from three subarctic lakes. *Journal of Geophysical Research: Biogeosciences*, *118*(3), 1307–1321. https://doi.org/10.1002/jgrg.20103

Wik, M., Thornton, B. F., Bastviken, D., MacIntyre, S., Varner, R. K., & Crill, P. M. (2014). Energy input is primary controller of methane bubbling in subarctic lakes. *Geophysical Research Letters*, *41*(2), 555–560. https://doi.org/10.1002/2013GL058510

Wik, M., Varner, R. K., Walter Anthony, K. M., MacIntyre, S., & Bastviken, D. (2016). Climate-sensitive northern lakes and ponds are critical components of methane release. *Nature Geoscience*, *9*(2), 99–105. https://doi.org/10.1038/ngeo2578

Wik, M., Thornton, B., Bastviken, D., Uhlbäck, J., & Crill, P. (2016). Biased sampling of methane release from northern lakes: A problem for extrapolation. *Geophysical Research Letters*, 43(3), 1256-1262. doi: 10.1002/2015gl066501

Woolway, R. I., & Merchant, C. J. (2019). Worldwide alteration of lake mixing regimes in response to climate change. *Nature Geoscience*, *12*(4), 271–276. https://doi.org/10.1038/s41561-019-0322-x

Woolway, R., Kraemer, B., Lenters, J., Merchant, C., O'Reilly, C. and Sharma, S. (2020). Global lake responses to climate change. Nature Reviews Earth & Environment, 1(8), pp.388-403.

Yamamoto, S., Alcauskas, J. B., & Crozier, T. E. (1976). Solubility of methane in distilled water and seawater. *Journal of Chemical & Engineering Data*, *21*(1), 78–80. https://doi.org/10.1021/je60068a029

Zeikus, J. G., & Winfrey, M. R. (1976). Temperature limitation of methanogenesis in aquatic sediments. *Applied and Environmental Microbiology*, *31*(1), 99 LP – 107. Retrieved from http://aem.asm.org/content/31/1/99.abstract

Zhang, Z., Zimmermann, N. E., Stenke, A., Li, X., Hodson, E. L., Zhu, G., … Poulter, B. (2017). Emerging role of wetland methane emissions in driving 21st century climate change. *Proceedings of the National Academy of Sciences*, *114*(36), 9647–9652. https://doi.org/10.1073/pnas.1618765114

Zhuang, Q., Melillo, J. M., Kicklighter, D. W., Prinn, R. G., McGuire, A. D., Steudler, P. A., … Hu, S. (2004). Methane fluxes between terrestrial ecosystems and the atmosphere at northern high latitudes during the past century: A retrospective analysis with a process-based biogeochemistry model. *Global Biogeochemical Cycles*, *18*(3). https://doi.org/10.1029/2004GB002239